


Gene body methylation regulates gene expression and mediates phenotypic diversity in natural *Arabidopsis* populations

Received: 21 February 2025

Accepted: 14 August 2025

Published online: 12 September 2025

 Check for updates

Zaigham Shahzad^{1,2}✉, Elizabeth Hollwey³, Jonathan D. Moore¹, Jaemyung Choi¹, Gaëlle Cassin-Ross^{4,5}, Hatem Rouached^{4,5}, Matthew R. Robinson³ & Daniel Zilberman^{1,3}✉

Genetic variation is generally regarded as a prerequisite for evolution. In principle, epigenetic information inherited independently of DNA sequence can also enable evolution, but whether this occurs in natural populations is unknown. Here we show that single-nucleotide and epigenetic gene body DNA methylation (gbM) polymorphisms explain comparable amounts of expression variance in *Arabidopsis thaliana* populations. We genetically demonstrate that gbM regulates transcription, and we identify and genetically validate many associations between gbM polymorphism and the variation of complex traits: fitness under heat and drought, flowering time and accumulation of diverse minerals. Epigenome-wide association studies pinpoint trait-relevant genes with greater precision than genetic association analyses, probably due to reduced linkage disequilibrium between gbM variants. Finally, we identify numerous associations between gbM epialleles and diverse environmental conditions in native habitats, suggesting that gbM facilitates adaptation. Overall, our results indicate that epigenetic methylation variation fundamentally shapes phenotypic diversity in a natural population.

The neo-Darwinian or modern synthesis at the centre of evolutionary biology¹ posits that DNA sequence changes are the substrate for evolution, with mechanisms such as natural selection and genetic drift shaping this variation to influence adaptation^{2,3}. Epigenetic information, which can be encoded independently of the DNA sequence, is essential for cell fate determination, development and environmental responses in eukaryotes^{4–7}. In theory, stably heritable epigenetic variation could contribute to adaptation^{8–12}. Epiallelic variation in many angiosperm genes, including *Linaria vulgaris* *Cyc*, tomato *CNR* and *VTE3*, maize *Spm*, rice *DI*, oil palm *MANTLED* and *Arabidopsis thaliana* *FWA*, *PAI2* and *IAA7*, influences traits^{13,14}. However, such epialleles are generally either

too unstable to influence a response to selection^{10–12} (such as *Cyc*¹⁵, *DI*¹⁶ and *MANTLED*¹⁷), have an underlying genetic basis (such as *PAI2*¹⁸ and *IAA7*¹⁴) or are artificial (such as *FWA*¹⁹ and *MANTLED*¹⁷) or evidence is lacking that heritable epiallelic variation occurs in nature (such as *CNR*²⁰, *VTE3*²¹, *Spm*²² and *DI*¹⁶). Furthermore, disentangling the effects of genetic and potentially epigenetic polymorphism in plant populations has proven difficult^{23,24}, with most polymorphism that might be epigenetic instead attributed to local (*cis*) or distant (*trans*) genetic polymorphism²⁵. Thus, the extent to which epigenetic inheritance mediates phenotypic diversity or influences evolutionary outcomes within natural populations is presently unclear^{13,25,26}.

¹Department of Cell and Developmental Biology, John Innes Centre, Norwich, UK. ²Department of Life Sciences, Syed Babar Ali School of Science and Engineering, Lahore University of Management Sciences, Lahore, Pakistan. ³Institute of Science and Technology, Klosterneuburg, Austria. ⁴Plant Resilience Institute, Michigan State University, East Lansing, MI, USA. ⁵Department of Plant, Soil, and Microbial Sciences, Michigan State University, East Lansing, MI, USA. ✉e-mail: zaigham.shahzad@lums.edu.pk; daniel.zilberman@ist.ac.at

DNA methylation can be epigenetically inherited over many generations^{13,27} and occurs in transposable elements (TEs) and bodies of transcribed genes^{28–31}. Plant TEs are methylated in all sequence contexts—CG, CHG and CHH (H being A, T or C)^{7,28,29,32}. TE methylation induces silencing³², confers genome stability^{31,33} and can influence the expression of neighbouring genes^{14,34–38}, and its variation has been associated with all known epialleles^{13,26}. Gene body methylation (gbM) occurs only in the CG context^{28,29,39}, although genes can also feature TE-like methylation in all contexts (teM)^{40,41}. TeM is associated with silencing^{30,40,41}, but the function of gbM has been extensively debated⁴². GbM is nearly ubiquitous in flowering plants^{43,44} and is common in animals^{28,29,45}. In both groups, gbM preferentially resides in nucleosome-wrapped DNA within the exons of conserved, constitutively transcribed genes^{30,46–49}. Conservation and phenomenological coherence suggest important functions⁴⁵. Indeed, gbM is associated with (small) gene expression differences within and between plant species^{24,41,50–53}, represses aberrant intragenic transcripts⁵⁴ and appears to be under natural selection^{51,52,55}. Moreover, loss of methyltransferase function causes developmental abnormalities in honeybees⁵⁶, animals in which methylation is principally restricted to gene bodies⁵⁷. However, gbM alteration has not been causatively linked to changes in gene expression in plants or animals^{30,58,59}, leading to the proposals that gbM is a non-functional and somewhat deleterious by-product of TE methylation (in plants)^{30,59,60} or has functions unrelated to gene expression (in animals)⁵⁸. Thus, the functional and evolutionary importance of gbM has been mysterious and controversial.

The *Arabidopsis* population exhibits extensive variation in TE methylation, gbM and teM^{40,41}. Methylation levels of natural accessions are associated with climate⁴⁰, suggesting that methylation variation could contribute to adaptation. Furthermore, genetically induced methylation polymorphism can account for the inheritance of complex *Arabidopsis* traits^{61–63}, and methylation changes have been linked to adaptation under artificial selection^{64,65}. Variation in TE methylation and teM has been repeatedly linked to genetic variation²⁶, but local gbM variation is primarily epigenetic^{41,66} and, hence, is a potential epigenetic mediator of phenotypic variation. However, natural methylation variation²⁴, and gbM variation specifically⁴⁰, were concluded to have limited contributions to gene expression variance in *Arabidopsis*. Thus, the extent to which variation of gbM or any other type of methylation underlies phenotypic diversity or drives the evolution of complex traits in natural populations is unknown¹³.

Results

GbM and teM are independent phenomena

Analyses of natural DNA methylation polymorphism in plant populations have not always strictly distinguished between gbM and teM, potentially motivated by the proposal that gbM is a by-product of teM⁵⁹. To evaluate the relationship between gbM and teM, we categorized genes of 948 *Arabidopsis* accessions into three distinct epigenetic states: unmethylated (UM), gbM and teM using published data⁴⁰ as previously described⁵⁴. In brief, genes containing segments of only CG methylation (mCG) in a given accession were classed as gbM in that accession, those containing non-CG methylation segments were classed as teM and those containing neither and with sufficient sequence coverage were classed as UM⁵⁴ (Supplementary Table 1 and Methods). Genes substantially overlapping both kinds of methylation segment (generally <1% of genes per accession) were classed as gbM and teM and excluded from further analyses. Considering unambiguously categorized genes, an accession contains on average 55% gbM genes, 33% UM genes and 12% teM genes (Fig. 1a). For example, the reference Col-0 accession has 56.5% gbM, 33.7% UM and 9.8% teM genes. Due to its variation, gbM is present in >90% of genes across the population (Supplementary Table 1). Consistent with published results^{40,51}, we find that gbM conservation varies across genes, falling into three main groups: gbM in >90% of accessions (41% of genes), gbM in ≤90% and

>10% of accessions (33%) and gbM in ≤10% of accessions (26%; Fig. 1b). Genes with high gbM population frequencies exhibit higher gbM levels that vary across a broader range (Extended Data Fig. 1a–d), as expected from the self-reinforcing gbM epigenetic dynamics⁶⁶. In contrast to gbM, the vast majority of genes exhibit teM in ≤10% of accessions (Fig. 1c), suggesting that teM is disfavoured in most genes, probably due to its negative effects on expression⁴⁰.

We find that the numbers of teM and gbM genes are very weakly (negatively) correlated across accessions (Fig. 1d) and are similarly weakly (positively) correlated under more restrictive definitions⁶⁰ of gbM and teM (Extended Data Fig. 1e). Genes with higher gbM conservation tend to be long and are robustly and broadly transcribed^{67,68}, the latter manifesting as high Shannon entropy (Extended Data Fig. 1f–h). By contrast, genes with higher teM conservation tend to be short and exhibit low expression and entropy (Extended Data Fig. 1f–h). TeM is most frequent in genes with low gbM conservation (Extended Data Fig. 1i–n). These results indicate that gbM and teM are prevalent in different types of genes and are not substantially associated. Consistently, a mathematical model that contains only gbM epigenetic dynamics accurately predicts gbM steady states and variation in *Arabidopsis*⁶⁶. Using this model, we can precisely predict the distribution of gbM levels within a core set of 6,736 gbM genes across the *Arabidopsis* population, including the frequency at which genes are UM (Fig. 1e). The model can even make the subtle distinction between genes with 100% gbM population frequency and those that are gbM in >99% but <100% of accessions (Fig. 1f,g). In essence, we can computationally recapitulate the epigenetic evolution of *Arabidopsis* gbM without recourse to teM. These results do not support the hypotheses that gbM originates as a by-product of teM⁵⁹ or that gbM promotes the transition to teM⁶⁰. Instead, our data indicate that intragenic gbM and teM are largely independent and should be treated separately, which is consistent with many lineages having only TE methylation (fungi and some land plants) or only gbM (many invertebrates)^{28–30}.

GbM and teM explain substantial amounts of gene expression variance

A study attempting to partition expression variance attributable to genome-wide methylation variation versus single-nucleotide polymorphisms (SNPs) within 135 *Arabidopsis* accessions found that the effects of either methylation or SNPs could appear marginal²⁴, presumably due to linkage disequilibrium between genetic and methylation polymorphisms⁶⁹. A recent maize study also found it difficult to disentangle methylation and genetic variation²³. To circumvent such limitations, we leveraged a statistical framework that robustly differentiates correlated variables⁷⁰ to partition expression variance attributable to common SNPs, gbM and teM mCG polymorphisms within 625 *Arabidopsis* accessions for which methylation and expression data are available⁴⁰.

We find that SNPs, gbM and teM explain substantial (and comparable) fractions of expression variance: SNPs explain 23.5% on average, gbM 15.2% and teM 26.0% (Fig. 2a). The variance attributable to SNPs is similar among genes with <90% gbM population frequency, with somewhat less variance explained in ≥90% gbM genes (Fig. 2b). By contrast, gbM explains considerably more expression variance as its population frequency increases (Fig. 2c). In genes with 100% gbM frequency, the effects of gbM (18.6%) and SNPs (20.6%) are nearly equal (Fig. 2b,c). TeM effects are bimodal (Fig. 2d), probably because they can be large but affect only a subset of genes due to teM rarity (Fig. 1a), so that teM expression effects are either substantial or effectively absent.

TeM explains more expression variance as gbM frequency decreases (Fig. 2d). Because we could only successfully model genes with low teM population frequencies (generally <3%; Supplementary Table 1), this effect is not due to differential *cis* teM prevalence. Instead, we find that teM explains more expression variance as Shannon entropy decreases (Fig. 2e), whereas gbM shows the opposite trend (Fig. 2f).

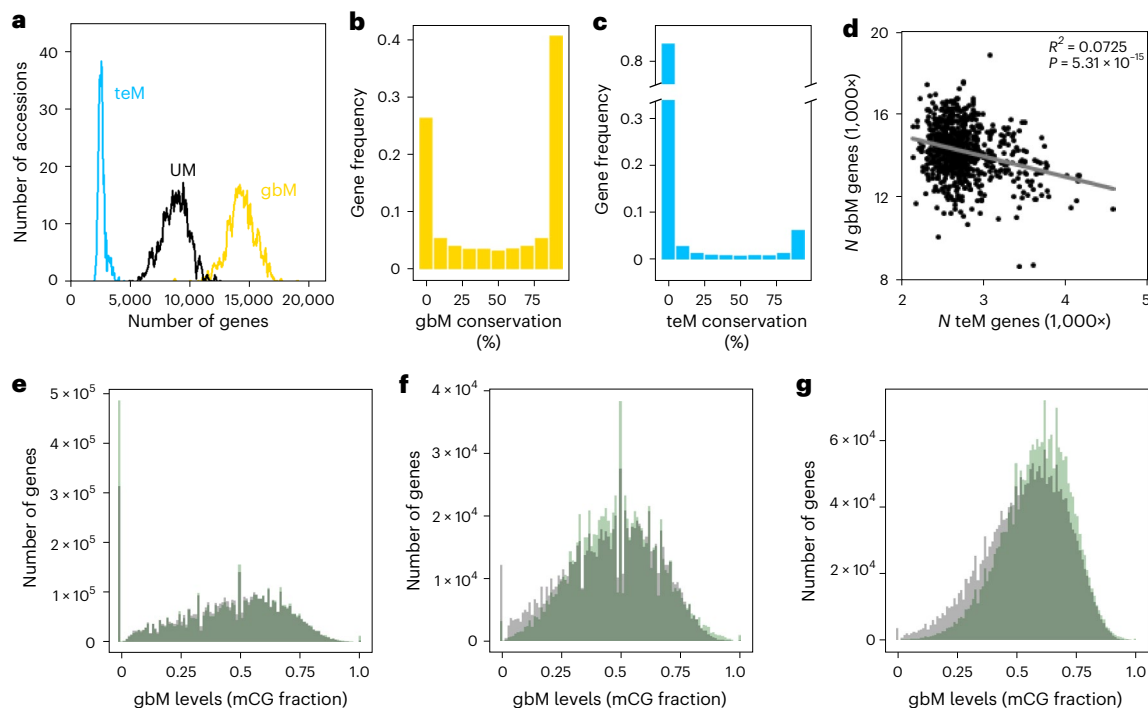


Fig. 1 | GbM and teM are independent phenomena. **a**, Frequency distributions of the number of genes classified as teM (blue), gbM (yellow) and UM (black) in 835 *Arabidopsis* accessions with >70% of genes called. **b,c**, Frequency distribution of gbM (**b**) and teM (**c**) conservation across 948 accessions within 24,465 genes with epigenetic state calls in >70% of accessions. **d**, Pearson's correlation analysis between the number (*N*) of gbM and teM genes across accessions. **e–g**, Simulated

(grey) and actual (green) mCG levels of all modelled genes ($N = 6,736$; **e**), genes with gbM frequency >99% and <100% in 740 accessions with global gbM similar to Col-0⁶⁶ ($N = 1,273$; **f**) and genes with 100% gbM frequency ($N = 2,942$; **g**), across the 740 accessions or 740 simulation iterations, so that **e**, for example, shows the distribution of -5 million ($6,736 \times 740$) empirical and -5 million simulated mCG data points.

We observe this even in genes with high gbM population frequencies (Fig. 2g,h), meaning that the trend is caused primarily by *trans* effects: gbM is more important for gene networks that regulate broadly and constitutively expressed genes, whereas teM is more important for networks regulating tissue-specific and inducible genes.

Although we find that teM and gbM explain substantial fractions of expression variance, the implications differ. Many *trans* genetic polymorphisms have been found to influence teM^{40,41,50,71,72}, and teM variation has been repeatedly linked with local genetic variation^{37,38,41}, especially structural variation (SV; insertions or deletions) caused by transposition. Hence, the extent to which teM variation is fundamentally epigenetic is unclear: much of it may be a readout for genetic variation. By contrast, although *trans* factors influence global gbM, local gbM variation is primarily caused by stochastic epigenetic fluctuations⁶⁶. Consistently, gbM levels of individual genes are weakly associated with global gbM levels across accessions ($R^2 < 0.1$ for ~80% genes; Extended Data Fig. 1o). Therefore, our gbM results indicate that much of the transcriptional variation in the *Arabidopsis* population is attributable to epigenetic inheritance.

Local intragenic methylation polymorphism is associated with transcriptional variance

The above analyses (Fig. 2) indicate that gene expression variance is influenced by methylation in natural populations, but do not distinguish *cis* and *trans* effects. To identify functional *cis* gbM and teM epialleles, we analysed associations between mCG and mRNA levels of individual genes. We identified 614 +eQTL^{gbM} genes (eQTL stands for expression quantitative trait locus) that show a positive association between gbM and gene expression and 148 -eQTL^{gbM} genes that exhibit a negative association at a conservative significance threshold (Bonferroni $\alpha = 0.05$); more eQTLs were identified at less stringent thresholds (Fig. 3a, Extended Data Fig. 2a and Supplementary Tables 2 and 3).

The dominance of positive associations between local gbM and expression variation (Extended Data Fig. 2b,c) is consistent with findings from previous studies^{24,41,50–53}. We find that eQTL^{gbM} genes are more likely to have had gbM before the speciation of *A. thaliana* than non-associated gbM (NA^{gbM}) genes⁵¹ (Extended Data Fig. 3a,b), suggesting that they are under selection to retain gbM. CG dinucleotide composition and length—hallmark features of gbM genes⁶⁰—are similar between eQTL^{gbM} and NA^{gbM} genes (Extended Data Fig. 3c–h), as are methylation patterns within and outside the genes (Extended Data Fig. 3i–n). However, gbM levels are slightly lower in +eQTL^{gbM} genes (Extended Data Fig. 3i,l), which also show lower expression (Extended Data Fig. 3e,h), suggesting that gbM may have more pronounced positive effects on gene expression when transcription is lower. In contrast to gbM, teM associations with expression are (as expected^{40,41}) overwhelmingly negative (Extended Data Fig. 2c,d and Supplementary Table 2), consistent with teM and gbM exerting different effects on transcription.

Given that genetic and epigenetic variation can be linked in the population⁷³, we investigated whether methylation variants influence expression independently of *cis*-acting DNA sequence changes. We identified *cis* SNPs associated with expression of the eQTL^{gbM/teM} Bonferroni genes, and retained eQTL^{gbM/teM} if significant associations between methylation and expression variation persisted after accounting for *cis* SNPs associated with expression (Supplementary Fig. 1). Nearly all -eQTL^{teM} were retained, as were >80% of +eQTL^{gbM}, and >60% of -eQTL^{gbM} and +eQTL^{teM} (Extended Data Fig. 4a,b and Supplementary Table 4). To account for residual confounding effects of SNPs, we defined SNP-invariant haplogroups for these genes and detected significant associations between mCG and gene expression for most eQTL^{gbM} and -eQTL^{teM} (Extended Data Fig. 4c–e and Supplementary Tables 5 and 6). Furthermore, we found the effects of known SV⁷⁴ on eQTL^{gbM} to be negligible (Extended Data Fig. 4f), whereas eQTL^{teM} are more often lost after accounting for SV (Extended Data Fig. 4g),

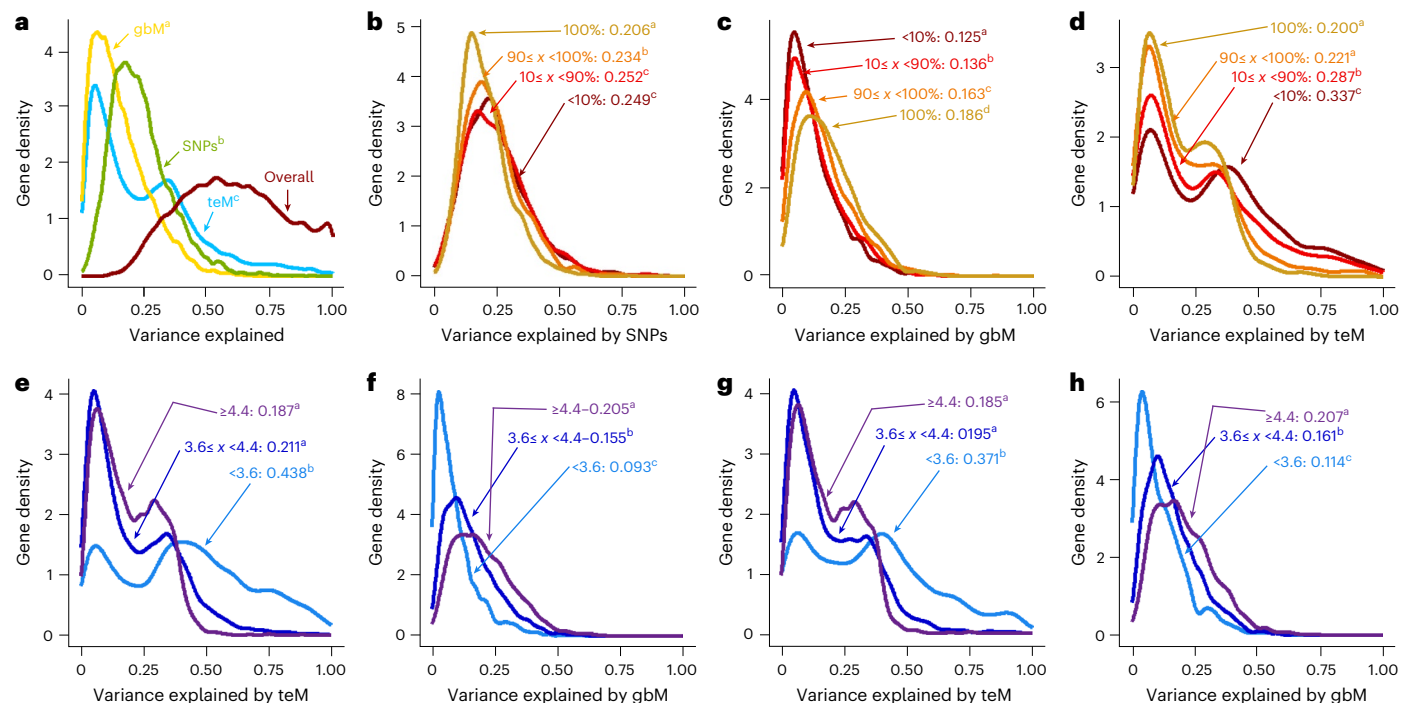


Fig. 2 | GbM and teM explain substantial amounts of gene expression variance.

a, Density plots grouping successfully modelled genes ($N = 7,339$) by the proportion of the expression variation explained by genome-wide gbM (gold), genome-wide teM (blue), SNPs (green) or all three (brown). **b–d**, Genes were split by their population gbM frequency ($<10\%$, $N = 1,970$; ≥ 10 and $<90\%$, $N = 1,508$; ≥ 90 and $<100\%$, $N = 1,970$; 100% , $N = 1,891$). The proportion of expression variation explained by SNPs (**b**), gbM (**c**) and teM (**d**) is plotted. **e,f**, Genes were split by Shannon entropy of expression (<3.6 , $N = 1,766$; $3.6–4.4$, $N = 3,584$; ≥ 4.4 ,

$N = 1,935$), and the proportion of expression variation explained by teM (**e**) and gbM (**f**) is plotted. **g,h**, GbM genes (gbM population frequency $\geq 90\%$) were split by Shannon entropy (<3.6 , $N = 427$; $3.6–4.4$, $N = 1,854$; ≥ 4.4 , $N = 1,564$) and the proportion of expression variation explained by teM (**g**) and gbM (**h**) is plotted. Superscript letters after mean values in all panels signify $P < 0.01$ using the non-parametric Kruskal–Wallis test followed by pairwise comparisons using the Wilcoxon rank-sum test with Bonferroni correction for multiple testing. Groups sharing the same letter are not significantly different.

consistent with the known association between teM variation and TE SV^{37,38,41}. In addition, we find that many (47.4%) retained eQTL^{teM} genes are affected by *trans* (presumably genetic) polymorphism (Extended Data Fig. 5a–c), which is consistent with published results^{40,41,50,71,72}. By contrast, *trans* genetic variation accounts for only ~1% of gbM variance within eQTL^{gbM} (Extended Data Fig. 5d–f and Methods). These findings support the conclusion that epigenetic gbM variation explains substantial gene expression variance in the *Arabidopsis* population, whereas teM variation is often a readout for *cis* or *trans* genetic polymorphism. This distinction highlights the importance of analysing gbM variation for understanding expression diversity within plant populations.

Loss of gbM quantitatively affects the expression of eQTL^{gbM} genes

To determine whether intragenic DNA methylation directly affects gene expression, we analysed published RNA sequencing (RNA-seq) data from *met1* mutants and wild-type (WT) controls across 16 natural *Arabidopsis* accessions⁷⁵. Inactivation of the *MET1* methyltransferase causes complete loss of gbM and nearly complete loss of mCG throughout the genome⁷⁶. WT methylated Bonferroni –eQTL^{teM} genes are strongly overexpressed in *met1* (Extended Data Fig. 6a), consistent with the established repressive activity of teM^{30,40,41}. As expected from the associations, Bonferroni +eQTL^{gbM} genes are modestly downregulated (expressed at ~88% of WT compared with NA^{gbM} controls), whereas –eQTL^{gbM} genes are modestly upregulated (expressed at ~109% of WT compared with NA^{gbM} controls; Fig. 3b). Analysis of additional Col-0 *met1* seedling⁵⁴, leaf⁵⁴ and inflorescence⁷⁷ RNA-seq datasets produced analogous results for –eQTL^{teM} and +eQTL^{gbM} genes, but –eQTL^{gbM} expression differences are not significant (probably due to the low number of these genes; Fig. 3c and Extended Data Fig. 6b–e).

Analysis of genes that passed less stringent significance thresholds produced similar results, albeit with decreased effect sizes (Extended Data Fig. 6f–i). Furthermore, +eQTL^{gbM} genes with higher mCG show stronger downregulation in *met1* RNA-seq data, whereas –eQTL^{gbM} genes with higher mCG exhibit stronger upregulation (Fig. 3d and Extended Data Fig. 6j,k), indicating that gbM quantitatively affects gene expression. The quantitative relationship between WT gbM and *met1* expression remains after removal of genes with methylation in the putative promoter (Extended Data Fig. 6l,m). Although *MET1* inactivation could influence gene expression by altering non-CG methylation and histone modifications⁷⁸, these chromatin features are not significantly changed in any relevant gbM gene category (Supplementary Fig. 2) and, thus, cannot explain our results.

The prevalence of gbM in constitutively expressed genes has motivated the proposal that gbM stabilizes gene expression by reducing transcriptional noise^{45,67,68,79,80}, so that gbM effects on mRNA levels could be interpreted as a secondary consequence. To test this, we analysed interreplicate variance within the *met1* and WT RNA-seq data from 16 *Arabidopsis* accessions⁷⁵. As expected, there is a strong negative correlation between transcriptional variability and gbM prevalence, but this remains the case in *met1* (Fig. 3e and Supplementary Fig. 3a). Variability is elevated in *met1*, but this effect is strongest in genes with low gbM, and decreases with gbM prevalence, including in eQTL^{gbM} genes (Fig. 3e,f and Supplementary Fig. 3). Given our observation that teM effects on expression also decrease with gbM prevalence (Fig. 2d), higher transcriptional variability in *met1* is probably caused by teM disruption. Therefore, any potential effects of gbM on transcriptional variability are low enough to be masked in *met1* data, whereas we can robustly detect gbM effects on steady-state mRNA levels in the same data (Fig. 3b,d and Extended Data Fig. 6f,g,j–m).

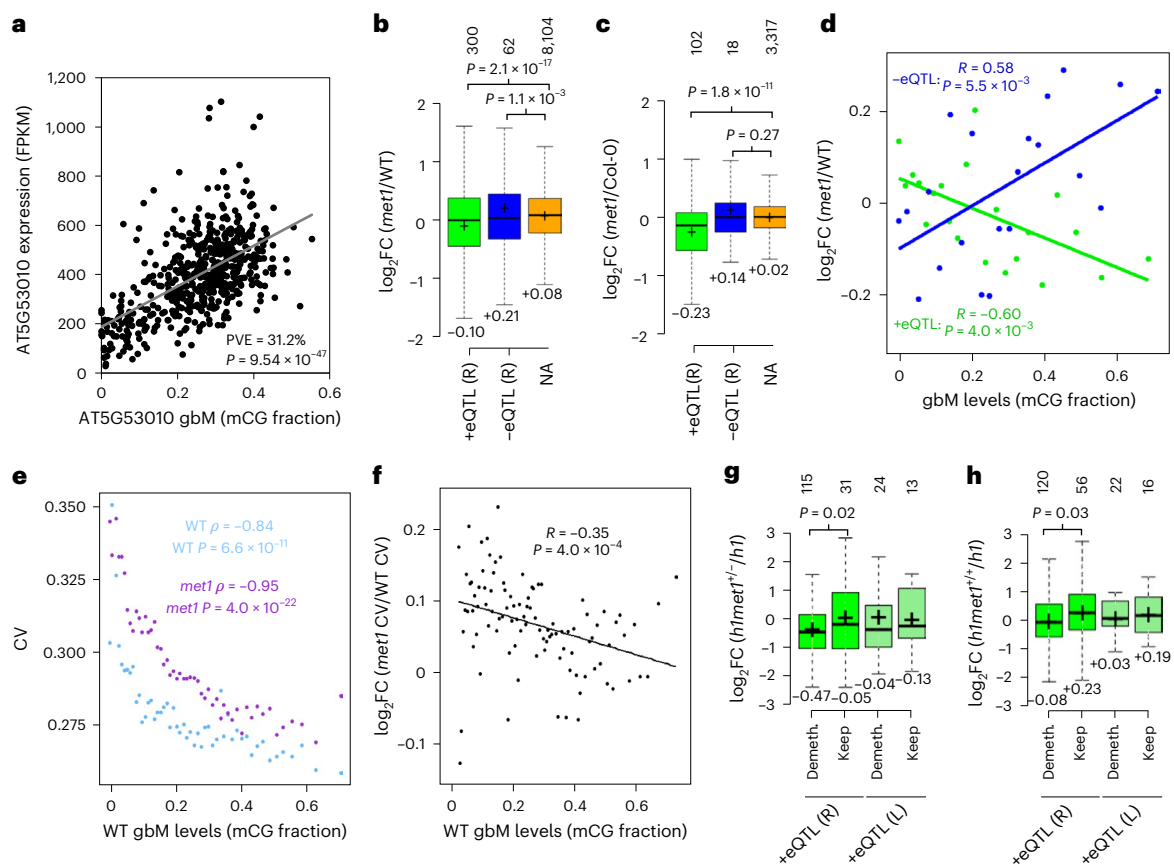


Fig. 3 | GbM quantitatively affects gene expression. **a**, GbM level and expression of *AT5G53010* across accessions. Per cent expression variance explained (PVE) by gbM is indicated. Pearson's correlation analysis was used to assess the association between the two variables. FPKM, fragments per kilobase of transcript per million mapped reads. **b, c**, Expression in *met1* seedlings compared with WT of Bonferroni ($\alpha = 0.05$) retained eQTL^{gbM} genes across 16 accessions (**b**) and across Col-0 tissues (leaf, seedling and inflorescence; **c**). Numbers of unique genes within each group are noted above the plots, means are indicated by '+' and noted below the plots. Sample medians are shown by centre lines, and box edges represent the 25th and 75th percentiles. Whiskers extend to 1.5 times the interquartile range. *P* values were calculated using a two-tailed Student's *t*-test to compare the indicated eQTL group with non-associated (NA) genes. **d**, Relationship between gbM levels of retained +eQTL^{gbM} and -eQTL^{gbM} genes in

WT plants across 16 accessions and log₂ fold expression change in *met1* compared with the WT of that accession. Genes were grouped by gbM levels. *R* and *P* values correspond to Pearson's correlation. **e**, Relationship between the gene expression coefficient of variation (CV) across biological replicates in WT (blue) and *met1* (purple) and WT gbM level across 16 accessions. Genes were grouped by gbM levels in WT. ρ and *P* values correspond to Spearman's rank correlation coefficient. **f**, Relationship between the log₂ fold CV change in *met1* compared with WT and the gbM level across 16 accessions. *R* and *P* values correspond to Pearson's correlation. **g, h**, Expression in *h1met1*^{+/+} (**g**) and *h1met1*^{+/+} (**h**) compared with *h1* of Bonferroni ($\alpha = 0.05$) retained (R) or lost (L) eQTL^{gbM} genes that are either demethylated (Demeth.) or keep methylation. Box plots as in **b** and **c**. *P*, two-tailed Student's *t*-test.

To further evaluate the direct impact of gbM loss on gene expression, we analysed a plant that is heterozygous for *met1* (*met1*^{+/+}) and has relatively normal TE methylation and limited gbM loss⁵⁴. This plant also contains loss-of-function mutations in two histone H1 genes⁵⁴; therefore, expression was analysed with respect to *h1*-mutant controls. We analysed only +eQTL^{gbM} genes, as we lacked statistical power for the smaller number of -eQTL^{gbM} genes. Retained +eQTL^{gbM} genes demethylated in this plant have significantly decreased (~35%) expression compared with retained +eQTL^{gbM} genes that maintain gbM (Fig. 3g), specifically linking gbM loss with reduced expression. To validate these findings, we isolated six *h1met1*^{+/+} progeny of *h1met1*^{+/+}. These plants exhibit mosaic demethylation of gbM genes, whereas TE methylation is comparatively normal (Supplementary Fig. 4). Retained +eQTL^{gbM} genes demethylated in *h1met1*^{+/+} plants display significantly reduced (~25%) expression compared with retained +eQTL^{gbM} genes that keep gbM (Fig. 3h). Altogether, we find that gbM loss consistently influences the expression of eQTL^{gbM} genes, regardless of the genetic background, tissue (seedlings, leaves or inflorescence), presence of functional *MET1*, or the extent of global teM or gbM perturbation. Therefore, our results establish gbM as a quantitative gene expression regulator.

GbM variation enables efficient identification of new functional genes

We find that methylation polymorphism explains a substantial amount of natural expression variance and directly affects gene expression (Figs. 2 and 3). This implies that methylation epialleles should drive trait variation in natural populations. To uncover how DNA methylation shapes natural phenotypic diversity, we performed epigenome-wide association (epiGWA) analyses between gbM or teM polymorphism and the variation of complex traits: relative fitness under different conditions⁸¹, 9 flowering time-related traits⁸² and the accumulation of 18 minerals in leaves⁸³. We identified 1 QTL^{gbM} for fitness in Madrid (hot climate) under low rainfall and high-density population growth (MLP), 8 QTL^{gbM} for flowering time traits and 19 QTL^{gbM} for leaf minerals (Supplementary Figs. 5–10, Supplementary Tables 7–13 and Methods). We also identified one QTL^{teM} for fitness in MLP conditions and six QTL^{teM} for mineral accumulation (Supplementary Figs. 5, 6 and 10 and Supplementary Tables 8 and 13). With the notable exception of two extensively studied flowering time genes—*FLC* and *FR1*⁸⁴—there was virtually no overlap between QTL^{gbM/teM} and genetic QTLs (Supplementary Figs. 6, 9 and 10 and Supplementary Tables 13–15),

suggesting distinct contributions of methylation variation to phenotypic diversity. Nonetheless, we found linkage disequilibrium⁶⁹ ($r = 0.725$, $D' = 0.824$, $P < 0.0001$) between *FRI* gbM and SNPs, suggesting that *FRI* epigenetic and genetic QTLs are redundant, and therefore we excluded *FRI* from further analyses.

We focused special attention on *FLC* (QTL^{gbM}) and the two MLP fitness QTLs—*Proline Transporter 1* (*PROT1*; *AT2G39890*; QTL^{gbM}) and *AT1G19410* (QTL^{teM})—because we identified *FLC* and *PROT1* as +eQTL^{gbM} and *AT1G19410* as a -eQTL^{teM} (Supplementary Table 3). Because multiple *FLC* SNP and SV alleles affect flowering time or vernalization response^{37,85,86}, we defined 13 *FLC* haplotypes that were invariant for SNPs and known SVs⁷⁴ (Supplementary Table 16), 12 of which contain gbM and UM accessions (Fig. 4a), suggesting complex gbM evolution at this locus. GbM accessions display significantly delayed flowering (flowering time at 16 °C, FT₁₆ °C) within five haplotypes (delay of >18 days in three haplotypes; Fig. 4a), and significantly higher *FLC* expression in three of these haplotypes (Fig. 4b). These results suggest that gbM promotes *FLC* expression, as expected for a +eQTL^{gbM}, and are consistent with the known function of *FLC* in delaying flowering⁸⁴. Although upstream teM has been linked to *FLC* expression and flowering time⁸⁷, exclusion of the relevant teM accessions does not alter our results, and in general we find that upstream teM is uncorrelated with *FLC* expression or flowering time (Supplementary Figs. 11–13). *FLC* is downregulated in *met1* regardless of WT methylation status (Extended Data Fig. 7a), suggesting indirect effects of global methylation loss.

For *PROT1* and *AT1G19410*, we found consistent associations between mCG, fitness, and expression after accounting for SV in the entire population, as well as in haplogroups invariant for SNPs and SVs (Extended Data Fig. 7b and Supplementary Table 16). As expected for a +eQTL^{gbM}, *PROT1* is downregulated by 38% in *met1* as determined by quantitative reverse transcription PCR (qRT-PCR; Extended Data Fig. 7c and Supplementary Table 17) and is downregulated in *met1* RNA-seq data from accessions in which *PROT1* is methylated (Extended Data Fig. 7d). *AT1G19410* teM is lost in plants that lack DRM and CMT methyltransferases (Extended Data Fig. 7e), and in such *ddcc* mutants⁸⁸ *AT1G19410* expression increases about sevenfold (Extended Data Fig. 7f and Supplementary Table 17), consistent with a -eQTL^{teM}.

The positive associations between fitness and mCG in *PROT1* and *AT1G19410* make clear predictions about the effects of gene inactivation: *PROT1* (+eQTL^{gbM}) inactivation should reduce fitness, whereas *AT1G19410* (-eQTL^{teM}) inactivation should enhance fitness. Genetic inactivation of *PROT1* indeed caused ~35% fitness reduction under joint heat and drought stress (Fig. 4c and Extended Data Fig. 8a). *PROT1*-mutant plants produced less biomass and had decreased survival to fruit, but had the same fecundity (seed set) as WT (Fig. 4d and Extended Data Fig. 8b–d). Consistently, *PROT1* gbM is specifically associated with survival in MLP conditions (Extended Data Fig. 8e–g). Inactivation of *AT1G19410* resulted in a slight (~13%) but non-significant increase in relative fitness under heat and drought stress (Extended Data Fig. 9a,b). However, *AT1G19410* mutants have greatly enhanced (>2-fold) fitness under heat stress alone, with >2-fold increased fecundity and significantly increased fertility (percentage of flowers developing siliques), but no major effect on survival or biomass (Extended Data Fig. 9b–f). Therefore, we named *AT1G19410* *ANAHITA* (*ANH*) after the ancient Persian goddess of fertility and water. Notably, the association of *ANH* teM is stronger with fecundity than survival in MLP conditions (Extended Data Fig. 9g–i). Thus, although both genes influence relative fitness, *PROT1* specifically influences survival, whereas *ANH* affects fecundity.

To more broadly examine the validity of epiGWA mapping, we analysed the six additional flowering time QTL^{gbM} genes, and ten QTL^{gbM} genes associated with accumulation of the most easily quantifiable minerals—potassium (K), magnesium (Mg), manganese (Mn) and zinc (Zn)—using T-DNA insertion mutants. We focused on

gbM QTLs because these are much more numerous and because gbM variation is unambiguously epigenetic. Mutants in all flowering time QTL^{gbM} genes except *AT3G43860* showed significantly altered FT₁₆ °C (Fig. 4e), and mutants in nine mineral QTL^{gbM} genes displayed significant changes in the accumulation of relevant minerals ($P \leq 0.07$, eight genes with $P \leq 0.03$; Fig. 4f–i). Thus, we validated nearly 90% (16/18, including the published *flc* flowering phenotype⁸⁹) of QTL^{gbM} via mutations in genes where gbM is associated with the trait. A comparative analysis of *Arabidopsis* SNP-based GWA studies across 48 diverse traits with 57 validated genes (Supplementary Table 18) revealed that the SNP with the lowest P value is located within the validated gene in only ~54% of cases (Fig. 4j). The high frequency of epiGWA pinpointing the trait-relevant gene is probably due to gbM epimutation rates exceeding genetic mutation rates by ~10⁵-fold^{66,90–92}. Such turnover should rapidly disrupt linkage between gbM polymorphism, so that only gbM in the causative gene is associated with trait variance. Given that the associations obtained with GWA and epiGWA analyses rarely overlap (Supplementary Figs. 6, 9 and 10), gbM-based epiGWA mapping presents a powerful and broadly applicable gene discovery tool, as we illustrate by identifying 15 new genes affecting six distinct phenotypes (MLP fitness, flowering time and accumulation of K, Mg, Mn and Zn).

GbM variation may facilitate local adaptation

Arabidopsis grows in a broad range of natural environments and shows extensive local adaptation⁹³. As we find that gbM polymorphism explains substantial gene expression variation, we tested whether gbM may facilitate adaptation by performing epiGWA analyses for 171 environmental variables⁹⁴. We detected 571 associations between 232 genes and 115 of these variables, with 77% of these associations not colocalizing with SNP associations (Extended Data Fig. 10a and Supplementary Table 19). Notably, gbM variation in 57 genes is associated with at least three environments, and P values for these genes are strongly correlated for associated environments (Fig. 5a,b and Supplementary Tables 19–21), suggesting that multiple correlated environmental conditions impose selection on epiallelic states of individual genes.

Our analysis identified several notable gbM associations with a plausible functional link to environmental adaptation (Fig. 5c–e and Extended Data Fig. 10b–d) that do not overlap with genetic associations (Supplementary Table 19). GbM variation in *CCS*, which mediates heat stress responses⁹⁵, is associated with summer insolation, with gbM epialleles more prevalent in high insolation environments (Fig. 5c). GbM in *CHY1*, which is involved in cold signalling and promotes freezing tolerance⁹⁶, is associated with spring minimum temperature, with gbM epialleles rare in environments where temperature drops below -4 °C (Fig. 5d). GbM in *HUP9*, a regulator of flooding stress response⁹⁷, is associated with annual precipitation (Extended Data Fig. 10b). *PYR1* gbM variation is associated with soil excess salts, with high-salt soils almost exclusively featuring gbM epialleles (Extended Data Fig. 10c). *PYR1* is an abscisic acid receptor⁹⁸, and abscisic acid is a central regulator of plant salt stress responses⁹⁹. GbM variation in the calcium sensor *SOS3*¹⁰⁰ associates with soil salinity and sodicity (Extended Data Fig. 10d), which includes calcium carbonate (CaCO₃) and gypsum (CaSO₄·2H₂O). Nearly all accessions from high-salinity and high-sodic soils have UM *SOS3* epialleles (Extended Data Fig. 10d). These findings suggest that natural gbM variation facilitates local adaptation in native habitats.

The most striking association we discovered is between *FLC* gbM and springtime concentration of nitrogen dioxide (NO₂), with UM *FLC* alleles prevalent in high-NO₂ environments (Fig. 5e and Supplementary Table 22). Because UM *FLC* accessions flower early (Fig. 4a), this association predicts that accessions from high-NO₂ environments should flower early. Indeed, flowering time (FT₁₆ °C) of laboratory grown *Arabidopsis* accessions is more strongly correlated with atmospheric NO₂ in native environments than with any other environmental variable (Fig. 5f and Supplementary Table 23). NO₂ levels vary regionally

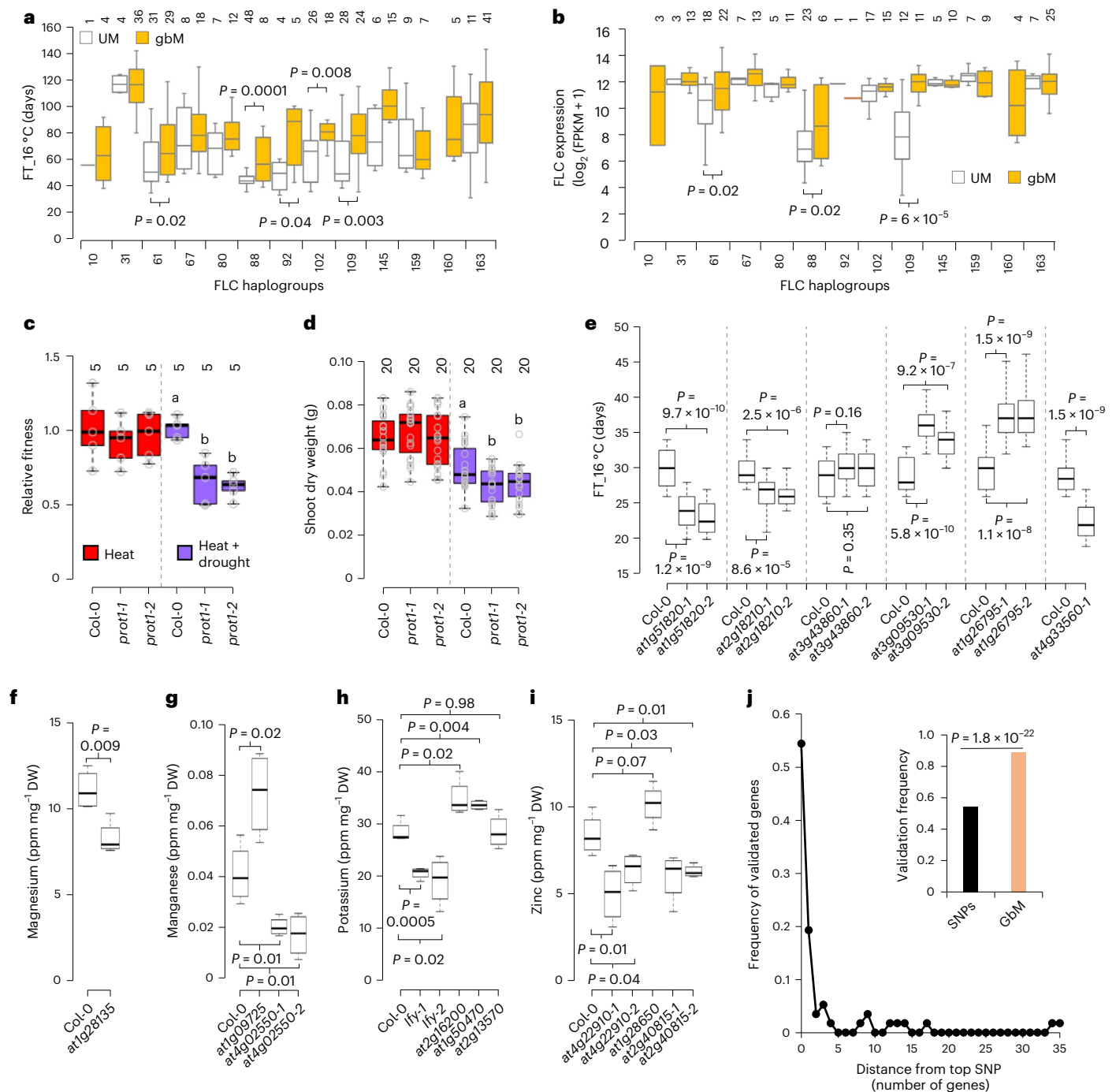
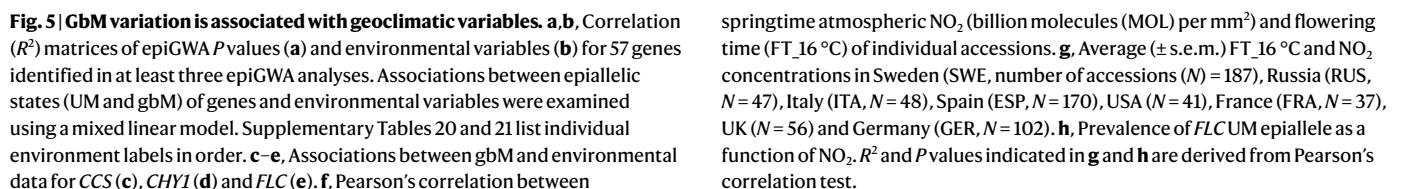


Fig. 4 | GbM variation enables efficient identification of new functional genes.

a, b, Association of FLC epiallelic states with $FT_{16}^{\circ C}$ (**a**) and FLC expression (**b**) in 13 FLC haplogroups invariant for SNPs and known SVs. Only accessions without TE polymorphism around FLC are considered. The number of accessions corresponding to each haplogroup are indicated. P values correspond to two-tailed Student's t -test. **c, d**, Fitness (**c**) or shoot dry weight (**d**) of *prot1* mutants (two independent alleles) relative to Col-0 under heat or joint heat and drought stress. Numbers of independent experiments are indicated for fitness (**c**), and plant numbers are indicated for shoot weight (**d**). Different letters signify $P < 0.05$, one-way analysis of variance, Tukey's test. **e**, Flowering time of Col-0 and knockout mutants of *AT1G51820*, *AT2G18210*, *AT3G43860*, *AT3G09530*, *AT1G26795* and *AT4G33560*. Plants were grown at $16^{\circ C}$. P values were calculated using a two-tailed t -test. **f–i**, Magnesium (**f**), manganese (**g**), potassium (**h**) and

zinc (**i**) levels of Col-0 and knockout mutants of *LEAFY*, *AT2G16200*, *AT1G50470*, *AT2G13570*, *AT4G22910*, *AT1G28650*, *AT2G40815*, *AT1G09725*, *AT4G02350* and *AT1G28135*. The number of biological replicates is 4. P values were calculated using a two-tailed t -test. Sample medians are represented by centre lines within the box plots (**a–i**). Box limits indicate the 25th and 75th percentiles; whiskers extend to 1.5 times the interquartile range. DW, dry weight. **j**, Distance (number of genes) of validated gene from the top SNP (SNP displaying the lowest association P value) in GWA analyses of various complex traits. Inset shows the frequency of top SNP located within the validated gene (encompassing the region from the end of the upstream gene to the beginning of the downstream gene) and the validation frequency for genes containing associated gbM variants. P values from the two-tailed Student's t -test comparing the two groups are shown.



Our findings reveal that gbM and teM are independent phenomena (Fig. 1) that explain substantial amounts of gene expression variation in the *Arabidopsis* population (Fig. 2). GbM is most important for broadly and constitutively expressed genes (Fig. 2f,h), consistent with its enrichment in such genes^{67,68}, whereas teM is most relevant for genes with narrow or inducible expression (Fig. 2e,g). We also find that gbM directly and quantitatively affects gene expression (Fig. 3),

and that its natural variation can be used to identify many new genes that influence a range of complex traits (Fig. 4). There is a great deal of gbM variation: just the core gbM genes analysed in Fig. 1e contain 299,679 polymorphic CG sites, compared with the 920,998 common SNPs across the *Arabidopsis* genome used in our analysis (Fig. 2). Thus—as for SNPs—many small effects can accumulate within gene networks to substantially influence gene expression (Fig. 2a–c). Overall, our results indicate that epigenetically variable gbM patterns are a major source of functional polymorphism in *Arabidopsis*.

Because DNA methylation is mutagenic¹⁰², and its presence in coding sequences probably incurs a fitness cost⁴⁵, the widespread conservation of gbM in plants and animals has presented a mystery. A potential explanation is that gbM variation can rapidly generate a range of gene expression epialleles, thereby accelerating adaptation to new or changing environments. The association between atmospheric NO₂, flowering time and *FLC* gbM (Fig. 5e–h) presents an illustration of how this might occur. Natural genetic variation at *FLC* is a major determinant of flowering time^{82,85,86} and is associated with over 20 environmental variables that are (or may plausibly be) related to flowering, including latitude, temperature and precipitation, but not NO₂ (ref. 94). The majority of atmospheric NO₂ (>75%) is produced by recent human activity, especially the burning of fossil fuel¹⁰³. Therefore, *Arabidopsis* populations have had to adapt to NO₂ concentrations (or a correlated unexamined environmental variable) changing over a few decades. Genetic adaptation at *FLC* apparently has not yet occurred in response to such rapid environmental alteration, or at least is too weak for detection. However, epigenetic gbM variation at *FLC* is significantly associated with atmospheric NO₂ (Fig. 5e–h), but not other environmental variables (Supplementary Table 22), which is consistent with our observation that *FLC* gbM and sequence variation are independent (Fig. 4a). Therefore, gbM variation at *FLC* has probably facilitated adaptation to anthropogenic NO₂ increases, whereas genetic variation has been involved in adaptation to environmental conditions that vary over longer timescales. This interplay between epigenetic and genetic adaptation is consistent with evolutionary models^{9–11} and may be a generally important component of environmental adaptation.

Methods

Methyl-C seq data analysis

Bisulfite sequence reads were accessed for the 1001 methylomes⁴⁰ experiments from the Sequence Read Archive (SRA) under accession number GSE43857. Sequencing reads of 948 non-redundant *Arabidopsis* accessions were aligned to the *Arabidopsis* TAIR10 genome reference sequence¹⁰⁴, using BSMAP¹⁰⁵ with default parameters, and known SNPs and indels⁸² were masked. Genes and transposons were annotated using the Araport11 annotation¹⁰⁶. Methylomes were segmented into UM, gbM and teM segments as previously described⁵⁴. The result of this segmentation is that gbM segments contain mCG anywhere between the annotated transcriptional start and termination sites of genes (and can span exons and/or introns) and lack non-CG methylation, teM segments contain non-CG methylation and UM segments lack methylation. Methylation of each CG site was called by comparing the counts of aligned reads indicating methylated and unmethylated status at the site. Fisher's exact test was used to determine whether there was sufficient read coverage at the site to distinguish the site from a fully unmethylated site with an error rate similar to the methylation rate observed in the chloroplast of the sample in question (as an estimate of bisulfite conversion inefficiency), or from a fully methylated site with a similar error rate. For sites where these tests indicated coverage was sufficient, a binomial test was used to identify sites with significantly more methylated reads than expected at an unmethylated site. Sites with significantly more methylated reads than would be expected for an unmethylated site, but with less than 45% reads methylated, were classified as partially methylated and generally treated as missing data. A gene was classified as gbM, teM,

both (gbM and teM), UM or indeterminate in each accession, based on overlapping methylome segments. Genes overlapped by a gbM segment three or more CG sites long, with at least one CG site called methylated by a binomial test, were classed as gbM genes, unless they are also overlapped by a teM segment at least 25% as long as the gbM segment, in which case they were classified as both. Genes overlapped by a teM segment three or more CG sites long were classified as teM genes, unless they are also overlapped by a gbM segment at least 25% as long as the teM segment, in which case they were classified as both. Genes not overlapped by gbM or teM segments and that span at least three sites called unmethylated by a binomial test were classified as UM. The remainder of genes were classified as indeterminate. Ambiguous genes (classified as 'both' or 'indeterminate') were discarded from further analysis. The mean CG methylation level of gbM or teM genes was calculated for each gene by summing the number of CG sites identified as methylated and dividing by the total number of CG sites classified as either methylated or unmethylated, as determined by a binomial test.

Estimation of prevalence of teM across gbM conservation bins

The number of genes having gbM or teM epigenetic states was determined in 948 *Arabidopsis* accessions. Pearson's correlation analysis for the number of gbM and teM genes was performed using accessions with more than 60% sequencing coverage of genomes. Conservation of epiallelic states of genes was analysed as a fraction of accessions having gbM or teM and the total available calls (that is, excluding accessions where the gene could not be called). Average prevalence of teM within gbM conservation bins was estimated in four gbM categories (0; >0% but <10%; 10–90%; and >90%), decile gbM bins and percentile gbM bins. To compare our results with published findings, identical analyses were performed using available data⁶⁰ with restrictive definitions of gbM and teM.

Methylation level distribution

Simulation of steady-state gbM was previously described⁶⁶. In brief, genic regions were refined by excluding sequences not methylated in the population or containing high levels of histone H2A.Z, which is known to antagonize DNA methylation¹⁰⁷. This resulted in a single, continuous methylatable region per gene for 7,980 genes⁶⁶. Further stringent filtering removed genes with a methylatable region covering less than 80% of the annotated gbM segment, refining the dataset to 6,736 genes. GbM within these loci was simulated from an entirely unmethylated starting state for 100,000 generations⁶⁶. To ensure robust comparison with natural variation, 740 iterations of the simulation were performed to produce a distribution of gbM levels for comparison with the empirical distribution over 740 accessions with global gbM levels similar to Col-0⁶⁶. Loci were grouped into percentiles by their gbM conservation level, with multiple data points for each gene showing mCG levels in different accessions or simulation iterations.

Partitioning expression variance attribution between gbM, teM and SNPs

RNA-seq data for 625 *Arabidopsis* accessions were retrieved from Gene Expression Omnibus (GEO): GSE80744 (ref. 1). Genes without detectable expression in leaves of >50% of accessions were discarded. To avoid confounding by low allele frequencies, we selected gbM and teM genes having at least one mCG site in >20% of accessions. This yielded a set of 10,206 genes with gbM polymorphism and 1,442 genes with teM polymorphism. From the imputation version of the 1001 genome SNP panel⁴, we selected common SNPs (frequency 15% and above), giving 920,998 SNPs. We then modelled the expression of each gene, y_j (a vector of length 625 accessions), as dependent upon the joint effects of gbM, X_{gbM} (a matrix with 625 rows and 10,206 columns), teM, X_{teM} (a matrix with 625 rows and 1,442 columns) and the SNPs, X_{snps} (a matrix with 625 rows and 920,998 columns), with the model

$$y_j = X_{gbM}b_{gbM} + X_{teM}b_{teM} + X_{snps}b_{snps} + \epsilon,$$

where b_{gbM} , b_{teM} and b_{snps} are regression coefficient vectors of length 10,206, 1,442 and 920,998 of the jointly estimated effects of gbM, teM and the SNPs, respectively, on the expression values of gene j . Each regression coefficient is modelled as coming from a mixture of normal distributions and a Dirac delta spike at zero. We fit this model using software for methylation data analysis that has been used extensively in human studies⁷⁰. GbM, teM and SNP effects are modelled as three independent groups with independent priors, where the total phenotypic variance attributable to each component is estimated from the data. Note that, while the groups have independent priors, each effect is modelled conditional on all other effects in the same group and all other groups. Altogether, we modelled 14,000 genes (genes need not have *cis* gbM or teM variance to be modelled, as the expression of each gene is modelled using the entire set of gbM, teM and SNPs). We checked convergence of the parameters across 5,000 posterior samples, discarding genes for which the analysis was highly divergent and retaining those (7,339; Supplementary Table 1) for which all parameters were estimated in a stable manner that was repeatable across multiple runs of the algorithm. Frequency distributions of the partitioned expression variance were generated via the kernel density estimation function in R.

Associations of intragenic DNA methylation with gene expression levels

RNA-seq data for 625 *Arabidopsis* accessions with gene-specific mCG levels were retrieved from GEO: [GSE80744](#) (ref. 40). Genes showing no detectable expression in leaves of any of these accessions were discarded from association analyses. Furthermore, to avoid confounding by low allele frequencies, these analyses were performed using gbM and teM genes having at least one mCG site in more than 10% *Arabidopsis* accessions. This allowed us to examine associations between mCG levels and gene expression for 18,679 gbM and 1,442 teM genes. Expression levels of genes were regressed on mCG levels in a linear model. Association P values for Pearson correlation were estimated using SigmaPlot 14.0.

Bonferroni ($\alpha = 0.05$) or 0.05 and 0.1 false discovery rate¹⁰⁸ (FDR) corrections were implemented to account for multiple tests. The percentage of expression variance explained by intragenic DNA methylation was calculated as

$$\text{PVE} = \frac{(\beta)^2 (V_{\text{mCG}})}{V_p},$$

where V_{mCG} is the variance of mCG, V_p corresponds to phenotypic (expression) variance and β effects for each association test were calculated as

$$\beta = Rx \left(\frac{\sigma_p}{\sigma_{\text{mCG}}} \right)$$

where R is Pearson's correlation coefficient, σ_p corresponds to standard deviation of gene expression and σ_{mCG} is standard deviation of mCG in the population.

Gene feature annotation

CG (CGG or CGT or CGC or CGA) sites were enumerated by scanning annotated genes¹⁰⁶ within the Col-0 reference sequence¹⁰⁴ with a three-base window and step size of one base. Gene lengths were obtained from the Col-0 annotation¹⁰⁶. Then, CG dinucleotide frequencies were calculated by normalizing the number of CG sites to a gene's annotated length. The mean expression level of each gene was calculated across 625 accessions. Shannon entropy data for 25,707 genes¹⁰⁹, ancestral genic methylation states⁵¹, and H3K9me2 and non-CG methylation data for *met1*-mutant plants compared with WT⁷⁸ were obtained from published sources.

Pipeline to account for SNP effects on the expression of eQTL^{gbM/teM} genes

To disentangle the effects of intragenic methylation on expression from *cis*-acting DNA sequence changes, we performed GWA analyses for the expression of 765 eQTL^{gbM} and 217 eQTL^{teM} Bonferroni genes using 1001 genomes SNP⁸² data in an accelerated mixed model¹¹⁰. Colocalization of each *cis* eQTL (eQTL^{SNP}) significant at Bonferroni threshold ($\alpha = 0.05$) with epigenetic eQTL was determined. The eQTL^{gbM/teM} genes for which no colocalized *cis* eQTL^{SNP} were detected are considered to affect gene expression variation independently of genetic variation (retained eQTL^{gbM/teM}) (Extended Data Fig. 4a,b and Supplementary Fig. 1). In cases where eQTLs^{gbM/teM} colocalized with eQTLs^{SNP}, the original population of accessions was separated into two nested populations, each fixed for the GWA SNP (Supplementary Fig. 1). Associations between intragenic DNA methylation and expression of these genes were reexamined within nested populations to account for the effects of SNP variation on expression. The genes that exhibited significant association between intragenic DNA methylation and expression in at least one nested population were also classified as retained eQTL^{gbM/teM}. Genes without significant associations between intragenic DNA methylation and gene expression in nested populations were considered probably confounded by linked SNPs in the population. Accordingly, these eQTL^{gbM/teM} were classified as lost eQTL^{gbM/teM} genes. To account for GWA SNP effects on expression variance, the per cent variance explained by methylation was calculated in nested populations as described above.

Analysis of published *met1* RNA-seq data

RNA-seq data for *met1* mutants were retrieved from [PRJEB54036](#) (ref. 75) for 16 different accessions of *Arabidopsis* (Aa-0, Baa-1, Bs-1, Bu-0, Col-0, Com-1, Cvi-0, Ei-2, Est-1, MAR2-3, Nok-3, Pi-0, Ste-0, Tscha-1, Tsu-0 and Uk-1). Reads were mapped to the genome using HiSat2, and changes in expression in comparison with WT across annotated genes (Araport11) identified using feature counts and DESeq2¹¹¹. Independent alleles of *met1* were analysed separately. Variability of these samples was calculated using the coefficient of variation of the TPM across three biological replicates separately for WT and *met1*. Only genes with detected reads in all biological replicates were used. Genes with no change in expression were additionally identified using DESeq2, selecting genes with an adjusted P value >0.05 and \log_2 expression change between -1 and 1 . Methylation levels for these accessions were extracted from the 1001 methylomes dataset⁴⁰, and gbM genes with mCG $>5\%$ spanning the transcription start site between -100 bp and 250 bp were excluded from expression analyses. Additional Col-0 datasets^{54,77} were retrieved from [GSE93584](#) and [GSE122394](#) for inflorescence, leaf and seedling, then aligned, and \log_2 FC was calculated as above.

Haplotype analyses

To account for allelic heterogeneity, associations between methylation and expression were examined within haplotypes. SNPs within and 4 kb upstream and downstream of genes were extracted from an imputed version of the 1001 genome SNP panel⁸². Sequences were aligned, and the accessions invariant for SNPs over the entire region for each gene were classified into a haplogroup. Haplogroups comprising fewer than 15 accessions were discarded from association analyses. Associations of mCG with gene expression or phenotypes were examined within haplogroups to fully account for the effects of local SNP variation on expression or phenotypic variation.

Accounting for SV effects on epigenetic QTLs

Structural variants were identified within epigenetic QTLs and 4 kb upstream and downstream using published TE polymorphism data in *Arabidopsis* accessions⁷⁴. Associations between structural polymorphism and expression were examined using a linear model and

the effects of structural variants on epigenetic QTLs were accounted through analysis in populations invariant for TE polymorphism⁷⁴.

EpiGWA studies for relative fitness

EpiGWA analyses for relative fitness were performed using published relative fitness data⁸¹ of 412 *Arabidopsis* accessions with sufficient mCG information. Common garden experiments had been performed in two climatically distinct field stations in Madrid (M) and Tübingen (T)⁸¹. Madrid presents a climate that transitions between Mediterranean and semi-arid climates and Tübingen is characterized by a temperate climate with no dry season and warm summers. High (H) and low (L) rainfall conditions typical of Tübingen and Madrid had been simulated during these experiments. To mimic low- and high-density populations in nature, individual (I) or multiple plants (P) had been grown in pots. EpiGWA analyses were performed using a linear model to assess associations between gbM or teM levels of genes and relative fitness. For these analyses, we focused on genes having gbM or teM conserved in more than 10% of *Arabidopsis* accessions. Linear model association mapping analyses may detect excessive significant marker-trait associations due to underlying population structure¹¹². We, however, detected only two associations (*PROT1* and AT1G19410) at 0.05 FDR for relative fitness in MLP (Supplementary Table 8). In addition, gbM variation in one gene *MuDR* (AT1G64255) is associated with relative fitness in MLI at 0.1 FDR. We next used quantile–quantile (QQ) plots and genomic control inflation factor λ (ref. 113) to assess confounding of association statistics (Supplementary Fig. 5 and Supplementary Table 7). λ was calculated using unlinked markers as

$$\lambda = \frac{\text{Median } X^2 \text{ observed } P}{\text{Median } X^2 \text{ expected } P},$$

where X^2 is the chi-square and P is the P value.

λ varied between phenotypes and ranged from 0.91 (relative fitness MHP (Madrid, High rainfall conditions, multiple Plants per pot)) to 1.48 (relative fitness TLI (Tübingen, Low rainfall conditions, Individual plants per pot)) (Supplementary Table 7). To control for confounding effects of population stratification, association statistics were corrected using λ , and the genome-wide significance threshold was recalculated using corrected P values. Both *PROT1* and AT1G19410 associations were significant at 0.05 FDR; however, *MuDR* was not significant at 0.1 FDR. Associations between intragenic DNA methylation and fitness significant at 0.05 FDR¹⁰⁸ are called epigenetic QTLs in this study. Tripartite associations between mCG levels, gene expression and relative fitness in MLP for *PROT1* and AT1G19410 were analysed using a linear model.

EpiGWA studies for flowering-related traits

Three types of epiGWA mapping were performed for flowering-related traits to identify the best model to account for confounding effects of population structure. A linear model was employed using mCG levels of genes, and two models, a generalized linear model (GLM) and a mixed linear model (MLM), were used for epiGWA using epiallelic states (UM or gbM; UM or teM) of genes. The methods for determination of epiallelic states of genes are described in the ‘Methyl-C seq data analysis’ section. The numbers of *Arabidopsis* accessions used for these epiGWA analyses are listed in Supplementary Table 9.

Linear model epiGWA mapping was performed to examine associations between mCG levels of genes (>10% gbM or teM conservation) and flowering time data (flowering time at 10 °C (FT₁₀ °C) and 16 °C (FT₁₆ °C))⁸². Association statistics for these epiGWA analyses were highly confounded ($\lambda = 4.50$ for FT₁₀ °C and $\lambda = 4.52$ for FT₁₆ °C; Supplementary Fig. 7 and Supplementary Table 10). Around 7,500 genes showed significant associations between mCG levels and flowering time at 0.05 FDR (Supplementary Fig. 7). Applying uniform λ correction for association P values in such cases is unsatisfactory for correcting

population structure at genes with strong differences in mCG levels across subpopulations and can also result in a loss of statistical power at genes with uniformly distributed mCG levels^{114,115}. Given the correlation of flowering with geographic regions, similar confounding of association statistics has been reported for flowering-related traits in *Arabidopsis* GWA studies¹¹². Strong confounding of P values renders linear model epiGWA using mCG levels inappropriate for association mapping in structured populations.

Next, we used binary epiallelic states of genes to perform GLM and MLM epiGWA mapping using FT₁₀ °C and FT₁₆ °C flowering time phenotypes and seven additional flowering-related phenotypes¹¹⁶ (number of days for inflorescence stalk to reach 1 cm, number of days to the opening of first flower, number of cauline leaves, number of rosette leaves, cauline branch number, primary number of inflorescence branches and length of primary inflorescence stalk). GLM implemented in TASSEL¹¹⁷ is a fixed-effects linear model that we used to test associations between epiallelic states and phenotypes. Association P values for several of the flowering phenotypes deviated significantly from expected distribution of P values, as indicated by QQ plots and λ estimates (Supplementary Fig. 8 and Supplementary Table 11). Hence, GLM using epiallelic states is also inappropriate for epiGWA mapping in structured populations. Next, an MLM¹¹⁷ that includes both fixed and random effects was used to correct population structure. MLM can be presented as

$$Y = \beta X + Zu + e,$$

where Y represents the vector of phenotypes, β denotes the vector containing fixed effects including genetic markers and population structure (Q matrix), u captures variance due to relatedness between individuals (kinship (K) matrix), X and Z are the design matrices and e captures variance due to the environment. The Q matrix of population membership estimates was derived from principal component analysis of epiallelic states. The K matrix accounts for epigenome-wide patterns of relatedness between the individuals and was estimated using the identity-by-state method¹¹⁷. QQ plots and λ estimates based on MLM epiGWA showed no significant deviation of distribution of association P values from null distributions (Supplementary Fig. 8 and Supplementary Table 11). MLM was thus used to dissect the epigenetic architecture of flowering-related phenotypes. Genes having methylation calls in <10% accessions were removed.

The association between epiallelic states and expression levels of eight flowering epiQTL genes was analysed using MLM epiGWA mapping. To examine associations between gene expression and phenotypes, flowering phenotypes were regressed on quantitative variation of gene expression in a linear model. Associations between epiallelic states and flowering or gene expression phenotypes in nested populations were tested using MLM epiGWA analyses.

EpiGWA studies for leaf mineral accumulation

Data for accumulation levels of 18 mineral elements⁸³ in leaves of 934 *Arabidopsis* accessions were used for epiGWA analyses to identify gbM and teM variants associated with the diversity of these traits. EpiGWA analyses were performed using MLM implemented in TASSEL¹¹⁷ as described above. We filtered out rare (minor allele frequency (MAF) <5%) gbM and teM variants. FDR 0.05 correction¹⁰⁸ was implemented to account for multiple tests and identify significant associations.

EpiGWA studies for geoclimatic variables

Data for 171 geoclimatic variables⁹⁴ were used for epiGWA analyses to identify gbM variants associated with environmental variation in the native range of *Arabidopsis* accessions. EpiGWA analyses were performed using MLM implemented in TASSEL¹¹⁷ as described above. We filtered out rare (MAF <5%) gbM variants. FDR 0.05 correction¹⁰⁸ was implemented to account for multiple tests and identify significant

associations. The density and distribution of *FLC*, *CHY1*, *CCS*, *HUP9*, *SOS3* and *PYRI* UM and gbM accessions was determined across the range of environmental variables.

Genome-wide association studies for relative fitness, flowering and mineral phenotypes

GWA analyses were performed for relative fitness in eight climates⁸¹, nine flowering-related phenotypes^{82,116} and levels of 18 minerals⁸³ using the same accessions as for epiGWA analyses. GWA mapping was carried out using 1001 genomes SNP data⁸² with an accelerated mixed model¹¹⁰ implemented in PyGWAS, a Python library for running GWAS (version 1.7.4). The accelerated mixed model has been shown to work well in previous studies for flowering and other phenotypes^{14,110,118}. SNPs with MAF >5% in the population were considered. An FDR correction of 0.05 (ref. 108) was implemented to account for multiple tests and identify genetic QTLs.

Genome-wide association to account for effects of *trans* QTLs on methylation variation

GWA analyses were performed for mCG levels of retained Bonferroni eQTL^{gbM/teM}. GWA mapping was carried out as described above to identify *trans* genetic QTLs that are significant at the Bonferroni threshold. These analyses were performed in three *Arabidopsis* populations: worldwide populations that we used for association mapping for gene expression and phenotypes, 133 accessions of the Swedish panel, in which strong *trans* effects were found for around 1,300 gbM genes⁵⁰, and a random non-Swedish worldwide population of equal size to the Swedish panel (Extended Data Fig. 5d–f). The percentage of mCG or epigenetic state variance explained by *trans* genetic QTLs was estimated as the ratio of sum of square of SNP markers (after fitting all other model terms) to the total sum of squares. If we consider only the 133 Swedish accessions, we find strong *trans* effects, with on average 37.9% of gbM variance explained at 11.5% of eQTL^{gbM} (4.4% gbM variance explained overall; Extended Data Fig. 5d–f). However, when we consider all 625 worldwide accessions, these *trans* effects nearly disappear; 9.7% of genes have significant *trans* QTLs, which on average explain 10.5% of gbM variance, with *trans* genetic variation accounting for only 1% of gbM variance over all tested eQTL^{gbM} (Extended Data Fig. 5). Notably, a panel of 133 randomly chosen worldwide accessions (same size as the Swedish panel) produced results that are almost identical to those of the Swedish panel and significantly different from the entire worldwide panel (Extended Data Fig. 5d–f). This indicates that estimates of *trans* effects on gbM variation are inflated in analyses of small populations, a phenomenon known as the Beavis effect^{119,120}.

RNA and bisulfite sequencing analysis of *h1* and *h1met1* mutants

Total RNA was extracted from 4-week-old *h1*^{−/−} and *h1*^{−/−};*met1*^{+/+} leaves using Trizol (Invitrogen, cat. no. 15596026). To remove genomic DNA (gDNA) from samples, 1 mg of RNA was treated with the DNA-free DNA removal kit (Thermo, AM1907). Then, 100 ng of gDNA-depleted total RNA was used to construct RNA-seq libraries with Ovation RNA-seq systems 1–16 for the model organism *Arabidopsis* (Nugen, cat. no. 0351). To investigate the association of intragenic DNA methylation with expression level in *h1*^{−/−};*met1*^{+/+} plants, we first defined demethylated gbM genes as ones with more than 10% CG methylation, lose more than 5% CG methylation in *h1*^{−/−};*met1*^{+/+} versus *h1*^{−/−} plants and have less than 5% CG methylation in *h1*^{−/−};*met1*^{+/+}. The gene expression fold change in *h1*^{−/−};*met1*^{+/+} plants (versus *h1*^{−/−} plants) was calculated using DeSeq2¹¹¹. To analyse the association between gene expression and gbM change, we compared the average expression fold change of demethylated gbM genes and gbM genes that retain intragenic DNA methylation in *h1*^{−/−};*met1*^{+/+} plants.

For *h1*^{−/−};*met1*^{+/+} plants isolated from segregating *h1*^{−/−};*met1*^{+/+}, 100–700 ng of DNA-depleted leaf RNA was used to construct RNA-seq

libraries (Illumina, cat. no. 20020610 and 20019792) following the manufacturer's manual. As segregating plants showed aberrant non-CG hypermethylation over gbM genes, we filtered out genes that gain non-CG methylation (average mCHG or mCHH > 0.01). GbM genes that either lose or keep methylation were identified as described for *h1*^{−/−};*met1*^{+/+}.

For bisulfite sequencing analysis of *h1*^{−/−};*met1*^{+/+} plants, we extracted gDNA from 4–5-week-old plant leaves. Then, 500 ng gDNA was sheared to 100–1,000 bp using Bioruptor Pico (Diagenode). gDNA libraries were constructed using NEBNext Ultra II DNA library prep kit for Illumina (New England Biolabs, cat. no. E7645). We performed bisulfite conversion twice (QIAGEN, cat. no. 59104) with ligated libraries and amplified libraries by PCR. Sequenced reads were mapped with the bs-seq pipeline (<https://zilbermanlab.net/tools/>).

RNA-seq and DNA methylation data are deposited in GEO with accession GSE183785.

Quantitative real-time PCR

Transcript levels of *PROT1* were quantified in Col-0 and *met1*-6¹⁰⁷ with plants grown in a chamber with cycles of 16 h light (120 μE m^{−2} s^{−1}) at 27 °C day and 16 °C night temperatures without humidity control, and shoots of 3-week-old plants were harvested. Each sample was a pool of five plant shoots, and samples were harvested from six independent experiments. For quantification of *AT1G19410* (*ANH*) mRNA levels, Col-0 and *ddcc*⁸⁸ plants were grown for 10 days as described above, then a 12-h cold treatment (4 °C) was applied to induce and detect the expression of *ANH*¹²¹. *ANH* transcript abundance was analysed from five independent experiments with 25 plant shoots pooled per experiment. Total RNA was extracted using the SV Total RNA Isolation System (Promega, cat. no. Z3101). One microgram of total RNA was used for first-strand cDNA synthesis using SuperScript IV Reverse Transcriptase (Invitrogen, 18090050) and Oligo(dT)15 Primer (Invitrogen, 18418012) in a final volume of 25 μl, according to the manufacturer's instructions. For qRT-PCR, 25 ng of first-strand cDNA was used as template. qRT-PCR was performed in triplicate using the CFX Connect Real Time PCR Detection System (Bio-Rad). cDNA amplification was monitored using SensiFAST SYBR No-ROX One-Step Kit (Biolone, Bio-72005) at an annealing temperature of 60 °C. *UBQ10* (AT4G05320) was used as an internal control. The primer sequences used for the analysis of *PROT1*, *ANH* and *UBQ10* are listed in Supplementary Table 17. Relative transcript levels (RTL) of genes of interest (GOI) compared with *UBQ10* were determined using the equation $RTL = [(E)^{-Ct}]^{GOI} / [(E)^{-Ct}]^{UBQ10}$.

Analysis of methylation upstream of *FLC*

Methylation was analysed upstream of *FLC* in reference to previously described regions 'X' and 'Y'⁶⁷ (Supplementary Fig. 11a). The borders of region X were set as 3,180,248–3,180,730 and the borders of region Y as 3,181,100–3,181,451. Region X was split into two separate regions (X1: 3,180,248–3,180,350 and X2: 3,180,351–3,180,730), as methylation of these regions showed different patterns of variation within the population (Supplementary Fig. 11a–d). Methylation levels in each region were calculated per accession. Only accessions with mean coverage over a given region of at least five reads per CG site and three reads each per CHG and CHH site were included for subsequent analysis. We identified 18 accessions methylated at X2 in all three contexts (>30% mCG, >5% mCHG and >1% mCHH; *Arabidopsis* accession IDs: 6092, 6102, 6111, 6136, 6137, 6145, 6150, 6907, 7430, 8247, 9524, 9703, 9759, 9777, 9790, 9839, 9850 and 9900). Of these, 13 belonged to haplogroups with multiple accessions (Supplementary Table 16). Flowering times and expression of *FLC* were available for 9 of these accessions (Supplementary Figs. 12e and 13e).

Quantification of minerals in plant samples

WT and mutant plants were grown in four biological replicates to analyse the accumulation of minerals in the shoots. Oven-dried samples (~15 mg) were placed in a vessel (Environmental Express, cat. no. SC415)

with 1 ml of nitric acid 65% (EMD Millipore cat. no. 1.00456.2500) and hydrogen peroxide 30% (Sigma-Aldrich cat. no. H3410-1L) and left at room temperature overnight. The samples were then digested using an Environmental Express Hotblock digestion system (cat. no. SC196) set at 80 °C for 8 h. Microwave-induced plasma optical emission spectrometer 4210 (MP-AES Agilent Technologies) coupled with an autosampler SPS4 (Agilent Technologies) was used to quantify K, Mg, Mn and Zn at 769.897 nm, 280.271 nm, 403.076 nm and 202.548 nm, respectively. Standard curves for each element were used to determine mineral concentrations in samples.

Plant materials, growth conditions and phenotyping

For relative fitness phenotyping under drought and heat stress, seeds of *Arabidopsis* Col-0 accessions and homozygous T-DNA insertion mutant lines for *PROT1* (*prot1-1*; SALK_030711C and *prot1-2*; SALK_018050C) and *ANH* (*anh-1*; SALK_098287C and *anh-2*; SALK_036488C) were obtained from Nottingham Arabidopsis Stock Centre. Seeds were stratified at 4 °C for 7 days and germinated in 9-cm pots containing vermiculite. Each pot contained four plants. Plants were grown in a chamber with cycles of 16 h light (120 $\mu\text{E m}^{-2} \text{s}^{-1}$) and 8 h dark, with 16 °C night and 27 °C day temperatures to induce heat stress. For well-watered conditions soil water content (SWC) was maintained at 60%, and 25% SWC was used for drought stress. Each pot was weighed daily to adjust SWC. Survival to fruit for Col-0 WT plants and *prot1* and *anh* mutant plants was scored before harvesting under heat or joint heat and drought stress. The number of seeds produced by surviving plants was recorded as a measure of fecundity. The fitness of each genotype under heat or combined heat and drought stress was calculated as a product of per cent survival and average fecundity during each experiment. The relative fitness of *prot1* and *anh* was estimated with respect to the average fitness of Col-0 within each condition. To understand the phenotypes that could contribute to differences in relative fitness of *prot1* and *anh* mutant plants, the three genotypes were phenotyped for shoot biomass and fertility. Shoot biomass for Col-0, *prot1* and *anh* plants was measured as shoot dry weight at maturity. Fertility was scored as a percentage of flowers producing siliques.

For flowering time phenotyping, seeds of *Arabidopsis* Col-0 accessions and homozygous T-DNA insertion mutant lines *AT1G51820* (*at1g51820-1*; SALK_208927 and *at1g51820-2*; SALK_055952), *AT1G18210* (*at1g18210-1*; GABI_826B09 and *at1g18210-2*; SALK_075633), *AT3G43860* (*at3g43860-1*; SALK_201540 and *at3g43860-2*; GABI_129G07), *AT3G09530* (*at3g09530-1*; SALK_034560 and *at3g09530-2*; SALK_023893), *AT1G26795* (*at1g26795-1*; SALK_124311 and *at1g26795-2*; SALK_124319) and *AT4G33560* (*at4g33560-1*; SALK_133653) were obtained from Nottingham Arabidopsis Stock Centre. T-DNA insertion mutant lines (*AT1G09725* (*at1g09725*; CS821762), *AT4G18370* (*at4g18370-1*; SALK_099162C and *at4g18370-2*; SALK_036606C), *AT4G02550* (*at4g02550-1*; SALK_136283C and *at4g02550-2*; SALK_028806C), *AT1G70920* (*at1g70920*; CS863888), *AT5G61850* (*lfy-1* and *lfy-9*), *AT2G16200* (*at2g16200*; SALK_082813), *AT1G50470* (*at1g50470*; SALK_200371C), *AT2G13570* (*at2g13570*; SALK_085886C), *AT4G22910* (*at4g22910-1*; SALK_083656C and *at4g22910-2*; SALK_101689C), *AT1G28650* (*at1g28650*; SALK_010911C), *AT2G40815* (*at2g40815-1*; SAIL_138_E02 and *at2g40815-2*; SALK_023214C) and *AT1G28135* (*at1g28135*; SALK_017094)) for mineral content analysis were obtained from Arabidopsis Biological Resource Center. Seeds were stratified at 4 °C for 7 days and germinated in 9-cm pots containing vermiculite, with each pot containing three plants. Plants were grown in a chamber with cycles of 16 h light (120 $\mu\text{E m}^{-2} \text{s}^{-1}$) and 8 h dark, with 16 °C constant temperature. The flowering time of each genotype was scored as the number of days to the appearance of the first flower.

Reporting summary

Further information on research design is available in the Nature Portfolio Reporting Summary linked to this article.

Data availability

Newly generated RNA-seq and bisulfite sequencing data from plants with mosaic gbM are available at GEO under accession number [GSE183785](#). In addition, previously published datasets were used as follows: [GSE43857](#): 1001 genomes project bisulfite sequencing data⁴⁰; [GSE80744](#): 1001 genomes project RNA-seq data⁴⁰; [PRJEB54036](#): RNA-seq *met1* mutant data from sixteen *Arabidopsis* accessions⁷⁵; [GSE122394](#): RNA-seq *met1* mutant data from Col-0 leaf and seedling⁵⁴; and [GSE93584](#): RNA-seq *met1* mutant data from Col-0 inflorescence⁷⁷.

References

- Bowler, P. J. in *Variation* (eds Hallgrímsson, B. & Hall, B. K.) 9–27 (Academic Press, 2005).
- Liu, Y. in *Advances in Genetics* (ed. Kumar, D.) vol. 102, 121–142 (Academic Press, 2018).
- Charlesworth, D., Barton, N. H. & Charlesworth, B. The sources of adaptive variation. *Proc. R. Soc. B* **284**, 20162864 (2017).
- Birnbaum, K. D. & Roudier, F. Epigenetic memory and cell fate reprogramming in plants. *Regeneration* **4**, 15–20 (2017).
- Elsherbiny, A. & Dobrev, G. Epigenetic memory of cell fate commitment. *Curr. Opin. Cell Biol.* **69**, 80–87 (2021).
- Greenberg, M. V. C. & Bourc'h, D. The diverse roles of DNA methylation in mammalian development and disease. *Nat. Rev. Mol. Cell Biol.* **20**, 590–607 (2019).
- Zhang, H., Lang, Z. & Zhu, J.-K. Dynamics and function of DNA methylation in plants. *Nat. Rev. Mol. Cell Biol.* **19**, 489–506 (2018).
- Bogan, S. N. & Yi, S. V. Potential role of DNA methylation as a driver of plastic responses to the environment across cells, organisms, and populations. *Genome Biol. Evol.* **16**, evae022 (2024).
- Kronholm, I. in *Handbook of Epigenetics (Third Edition)* (ed. Tollefsbol, T. O.) 551–565 (Academic Press, 2023).
- Gómez-Schiavon, M. & Buchler, N. E. Epigenetic switching as a strategy for quick adaptation while attenuating biochemical noise. *PLoS Comput. Biol.* **15**, e1007364 (2019).
- Kronholm, I. & Collins, S. Epigenetic mutations can both help and hinder adaptive evolution. *Mol. Ecol.* **25**, 1856–1868 (2016).
- Slatkin, M. Epigenetic inheritance and the missing heritability problem. *Genetics* **182**, 845–850 (2009).
- Quadrana, L. & Colot, V. Plant transgenerational epigenetics. *Annu. Rev. Genet.* **50**, 467–491 (2016).
- Shahzad, Z., Eaglesfield, R., Carr, C. & Amtmann, A. Cryptic variation in RNA-directed DNA-methylation controls lateral root development when auxin signalling is perturbed. *Nat. Commun.* **11**, 218 (2020).
- Cubas, P., Vincent, C. & Coen, E. An epigenetic mutation responsible for natural variation in floral symmetry. *Nature* **401**, 157–161 (1999).
- Miura, K. et al. A metastable DWARF1 epigenetic mutant affecting plant stature in rice. *Proc. Natl Acad. Sci. USA* **106**, 11218–11223 (2009).
- Ong-Abdullah, M. et al. Loss of Karma transposon methylation underlies the mantled somaclonal variant of oil palm. *Nature* **525**, 533–537 (2015).
- Melquist, S., Luff, B. & Bender, J. *Arabidopsis* PAI gene arrangements, cytosine methylation and expression. *Genetics* **153**, 401–413 (1999).
- Soppe, W. J. J. et al. The late flowering phenotype of FWA mutants is caused by gain-of-function epigenetic alleles of a homeodomain gene. *Mol. Cell* **6**, 791–802 (2000).
- Manning, K. et al. A naturally occurring epigenetic mutation in a gene encoding an SBP-box transcription factor inhibits tomato fruit ripening. *Nat. Genet.* **38**, 948–952 (2006).
- Quadrana, L. et al. Natural occurring epialleles determine vitamin E accumulation in tomato fruits. *Nat. Commun.* **5**, 4027 (2014).

22. Fedoroff, N., Schläppli, M. & Raina, R. Epigenetic regulation of the maize Spm transposon. *BioEssays* **17**, 291–297 (1995).
23. Xu, G. et al. Evolutionary and functional genomics of DNA methylation in maize domestication and improvement. *Nat. Commun.* **11**, 5539 (2020).
24. Meng, D. et al. Limited contribution of DNA methylation variation to expression regulation in *Arabidopsis thaliana*. *PLoS Genet.* **12**, e1006141 (2016).
25. Baduel, P. et al. The evolutionary consequences of interactions between the epigenome, the genome and the environment. *Evol. Appl.* **17**, e13730 (2024).
26. Baduel, P. & Colot, V. The epiallelic potential of transposable elements and its evolutionary significance in plants. *Philos. Trans. R. Soc. B* **376**, 20200123 (2021).
27. Heard, E. & Martienssen, R. A. Transgenerational epigenetic inheritance: myths and mechanisms. *Cell* **157**, 95–109 (2014).
28. Zemach, A., McDaniel, I. E., Silva, P. & Zilberman, D. Genome-wide evolutionary analysis of eukaryotic DNA methylation. *Science* **328**, 916–919 (2010).
29. Feng, S. et al. Conservation and divergence of methylation patterning in plants and animals. *Proc. Natl Acad. Sci. USA* **107**, 8689–8694 (2010).
30. Bewick, A. J. & Schmitz, R. J. Gene body DNA methylation in plants. *Curr. Opin. Plant Biol.* **36**, 103–110 (2017).
31. Jones, P. A. Functions of DNA methylation: islands, start sites, gene bodies and beyond. *Nat. Rev. Genet.* **13**, 484–492 (2012).
32. Law, J. A. & Jacobsen, S. E. Establishing, maintaining and modifying DNA methylation patterns in plants and animals. *Nat. Rev. Genet.* **11**, 204–220 (2010).
33. Du, J., Johnson, L. M., Jacobsen, S. E. & Patel, D. J. DNA methylation pathways and their crosstalk with histone methylation. *Nat. Rev. Mol. Cell Biol.* **16**, 519–532 (2015).
34. Qiu, Y. & Köhler, C. Mobility connects: transposable elements wire new transcriptional networks by transferring transcription factor binding motifs. *Biochem. Soc. Trans.* **48**, 1005–1017 (2020).
35. Hollister, J. D. & Gaut, B. S. Epigenetic silencing of transposable elements: a trade-off between reduced transposition and deleterious effects on neighboring gene expression. *Genome Res.* **19**, 1419–1428 (2009).
36. Hollister, J. D. et al. Transposable elements and small RNAs contribute to gene expression divergence between *Arabidopsis thaliana* and *Arabidopsis lyrata*. *Proc. Natl Acad. Sci. USA* **108**, 2322–2327 (2011).
37. Quadrana, L. et al. The *Arabidopsis thaliana* mobilome and its impact at the species level. *eLife* **5**, e15716 (2016).
38. Stuart, T. et al. Population scale mapping of transposable element diversity reveals links to gene regulation and epigenomic variation. *eLife* **5**, e20777 (2016).
39. Yan, H. et al. DNA methylation in social insects: how epigenetics can control behavior and longevity. *Annu. Rev. Entomol.* **60**, 435–452 (2015).
40. Kawakatsu, T. et al. Epigenomic diversity in a global collection of *Arabidopsis thaliana* accessions. *Cell* **166**, 492–505 (2016).
41. Schmitz, R. J. et al. Patterns of population epigenomic diversity. *Nature* **495**, 193–198 (2013).
42. Muyle, A. M., Seymour, D. K., Lv, Y., Huettel, B. & Gaut, B. S. Gene body methylation in plants: mechanisms, functions, and important implications for understanding evolutionary processes. *Genome Biol. Evol.* **14**, evac038 (2022).
43. Niederhuth, C. E. et al. Widespread natural variation of DNA methylation within angiosperms. *Genome Biol.* **17**, 194 (2016).
44. Takuno, S., Ran, J.-H. & Gaut, B. S. Evolutionary patterns of genic DNA methylation vary across land plants. *Nat. Plants* **2**, 15222 (2016).
45. Zilberman, D. An evolutionary case for functional gene body methylation in plants and animals. *Genome Biol.* **18**, 87 (2017).
46. Lyons, D. B. & Zilberman, D. DDM1 and Lsh remodelers allow methylation of DNA wrapped in nucleosomes. *eLife* **6**, e30674 (2017).
47. Lewis, S. H. et al. Widespread conservation and lineage-specific diversification of genome-wide DNA methylation patterns across arthropods. *PLoS Genet.* **16**, e1008864 (2020).
48. Dixon, G. B., Bay, L. K. & Matz, M. V. Evolutionary consequences of DNA methylation in a basal metazoan. *Mol. Biol. Evol.* **33**, 2285–2293 (2016).
49. Bräutigam, K. & Cronk, Q. DNA methylation and the evolution of developmental complexity in plants. *Front. Plant Sci.* **9**, 1447 (2018).
50. Dubin, M. J. et al. DNA methylation in *Arabidopsis* has a genetic basis and shows evidence of local adaptation. *eLife* **4**, e05255 (2015).
51. Muyle, A., Ross-Ibarra, J., Seymour, D. K. & Gaut, B. S. Gene body methylation is under selection in *Arabidopsis thaliana*. *Genetics* <https://doi.org/10.1093/genetics/iyab061> (2021).
52. Seymour, D. K. & Gaut, B. S. Phylogenetic shifts in gene body methylation correlate with gene expression and reflect trait conservation. *Mol. Biol. Evol.* **37**, 31–43 (2020).
53. Takuno, S., Seymour, D. K. & Gaut, B. S. The evolutionary dynamics of orthologs that shift in gene body methylation between *Arabidopsis* species. *Mol. Biol. Evol.* **34**, 1479–1491 (2017).
54. Choi, J., Lyons, D. B., Kim, M. Y., Moore, J. D. & Zilberman, D. DNA methylation and Histone H1 jointly repress transposable elements and aberrant intragenic transcripts. *Mol. Cell* **77**, 310–323.e7 (2020).
55. Takuno, S. & Gaut, B. S. Gene body methylation is conserved between plant orthologs and is of evolutionary consequence. *Proc. Natl Acad. Sci. USA* **110**, 1797–1802 (2013).
56. Kucharski, R., Maleszka, J., Foret, S. & Maleszka, R. Nutritional control of reproductive status in honeybees via DNA methylation. *Science* **319**, 1827–1830 (2008).
57. Harris, K. D., Lloyd, J. P. B., Domb, K., Zilberman, D. & Zemach, A. DNA methylation is maintained with high fidelity in the honey bee germline and exhibits global non-functional fluctuations during somatic development. *Epigenet. Chromatin* **12**, 62 (2019).
58. Bewick, A. J. et al. Dnmt1 is essential for egg production and embryo viability in the large milkweed bug, *Oncopeltus fasciatus*. *Epigenet. Chromatin* **12**, 6 (2019).
59. Bewick, A. J. et al. On the origin and evolutionary consequences of gene body DNA methylation. *Proc. Natl Acad. Sci. USA* **113**, 9111–9116 (2016).
60. Zhang, Y., Wendte, J. M., Ji, L. & Schmitz, R. J. Natural variation in DNA methylation homeostasis and the emergence of epialleles. *Proc. Natl Acad. Sci. USA* **117**, 4874–4884 (2020).
61. Cortijo, S. et al. Mapping the epigenetic basis of complex traits. *Science* **343**, 1145–1148 (2014).
62. Johannes, F. et al. Assessing the impact of transgenerational epigenetic variation on complex traits. *PLoS Genet.* **5**, e1000530 (2009).
63. Furci, L. et al. Identification and characterisation of hypomethylated DNA loci controlling quantitative resistance in *Arabidopsis*. *eLife* **8**, e40655 (2019).
64. Schmid, M. W. et al. Contribution of epigenetic variation to adaptation in *Arabidopsis*. *Nat. Commun.* **9**, 4446 (2018).
65. Kronholm, I., Bassett, A., Baulcombe, D. & Collins, S. Epigenetic and genetic contributions to adaptation in *Chlamydomonas*. *Mol. Biol. Evol.* **34**, 2285–2306 (2017).
66. Briffa, A. et al. Millennia-long epigenetic fluctuations generate intragenic DNA methylation variance in *Arabidopsis* populations. *Cell Syst.* <https://doi.org/10.1016/j.cels.2023.10.007> (2023).
67. Zhang, X. et al. Genome-wide high-resolution mapping and functional analysis of DNA methylation in *Arabidopsis*. *Cell* **126**, 1189–1201 (2006).

68. Zilberman, D., Gehring, M., Tran, R. K., Ballinger, T. & Henikoff, S. Genome-wide analysis of *Arabidopsis thaliana* DNA methylation uncovers an interdependence between methylation and transcription. *Nat. Genet.* **39**, 61–69 (2007).
69. Flint-Garcia, S. A., Thornsberry, J. M. & Buckler, E. S. Structure of linkage disequilibrium in plants. *Annu. Rev. Plant Biol.* **54**, 357–374 (2003).
70. Trejo Banos, D. et al. Bayesian reassessment of the epigenetic architecture of complex traits. *Nat. Commun.* **11**, 2865 (2020).
71. Shen, X. et al. Natural CMT2 variation is associated with genome-wide methylation changes and temperature seasonality. *PLoS Genet.* **10**, e1004842 (2014).
72. Sasaki, E., Kawakatsu, T., Ecker, J. R. & Nordborg, M. Common alleles of CMT2 and NRPE1 are major determinants of CHH methylation variation in *Arabidopsis thaliana*. *PLoS Genet.* **15**, e1008492 (2019).
73. Stefansson, O. A. et al. The correlation between CpG methylation and gene expression is driven by sequence variants. *Nat. Genet.* **56**, 1624–1631 (2024).
74. Baduel, P. et al. Genetic and environmental modulation of transposition shapes the evolutionary potential of *Arabidopsis thaliana*. *Genome Biol.* **22**, 138 (2021).
75. Srikant, T. et al. Canalization of genome-wide transcriptional activity in *Arabidopsis thaliana* accessions by MET1-dependent CG methylation. *Genome Biol.* **23**, 263 (2022).
76. Catoni, M. et al. DNA sequence properties that predict susceptibility to epiallelic switching. *EMBO J.* **36**, 617–628 (2017).
77. Oberlin, S., Sarazin, A., Chevalier, C., Voinnet, O. & Mari-Ordóñez, A. A genome-wide transcriptome and translome analysis of *Arabidopsis* transposons identifies a unique and conserved genome expression strategy for Ty1/Copia retroelements. *Genome Res.* **27**, 1549–1562 (2017).
78. Deleris, A. et al. Loss of the DNA methyltransferase MET1 induces H3K9 hypermethylation at PcG target genes and redistribution of H3K27 trimethylation to transposons in *Arabidopsis thaliana*. *PLoS Genet.* **8**, e1003062 (2012).
79. Zastapilo, J. et al. Gene body methylation buffers noise in gene expression in plants. Preprint at *bioRxiv* <https://doi.org/10.1101/2024.07.01.601483> (2024).
80. Horvath, R., Laenen, B., Takuno, S. & Slotte, T. Single-cell expression noise and gene-body methylation in *Arabidopsis thaliana*. *Heredity* **123**, 81–91 (2019).
81. Exposito-Alonso, M., Burbano, H. A., Bossdorf, O., Nielsen, R. & Weigel, D. Natural selection on the *Arabidopsis thaliana* genome in present and future climates. *Nature* **573**, 126–129 (2019).
82. The 1001 Genomes Consortium. 1,135 genomes reveal the global pattern of polymorphism in *Arabidopsis thaliana*. *Cell* **166**, 481–491 (2016).
83. Campos, A. C. A. L. et al. 1,135 ionomes reveal the global pattern of leaf and seed mineral nutrient and trace element diversity in *Arabidopsis thaliana*. *Plant J.* **106**, 536–554 (2021).
84. Maple, R., Zhu, P., Hepworth, J., Wang, J.-W. & Dean, C. Flowering time: from physiology, through genetics to mechanism. *Plant Physiol.* **195**, 190–212 (2024).
85. Hepworth, J. et al. Natural variation in autumn expression is the major adaptive determinant distinguishing *Arabidopsis* FLC haplotypes. *eLife* **9**, e57671 (2020).
86. Li, P. et al. Multiple FLC haplotypes defined by independent cis-regulatory variation underpin life history diversity in *Arabidopsis thaliana*. *Genes Dev.* **28**, 1635–1640 (2014).
87. Williams, B. P., Bechen, L. L., Pohlmann, D. A. & Gehring, M. Somatic DNA demethylation generates tissue-specific methylation states and impacts flowering time. *Plant Cell* **34**, 1189–1206 (2022).
88. Stroud, H. et al. Non-CG methylation patterns shape the epigenetic landscape in *Arabidopsis*. *Nat. Struct. Mol. Biol.* **21**, 64–72 (2014).
89. Berry, S., Hartley, M., Olsson, T. S. G., Dean, C. & Howard, M. Local chromatin environment of a Polycomb target gene instructs its own epigenetic inheritance. *eLife* **4**, e07205 (2015).
90. Becker, C. et al. Spontaneous epigenetic variation in the *Arabidopsis thaliana* methylome. *Nature* **480**, 245–249 (2011).
91. Schmitz, R. J. et al. Transgenerational epigenetic instability is a source of novel methylation variants. *Science* **334**, 369–373 (2011).
92. Van der Graaf, A. et al. Rate, spectrum, and evolutionary dynamics of spontaneous epimutations. *Proc. Natl Acad. Sci. USA* **112**, 6676–6681 (2015).
93. Ågren, J. & Schemske, D. W. Reciprocal transplants demonstrate strong adaptive differentiation of the model organism *Arabidopsis thaliana* in its native range. *New Phytol.* **194**, 1112–1122 (2012).
94. Ferrero-Serrano, Á. & Assmann, S. M. Phenotypic and genome-wide association with the local environment of *Arabidopsis*. *Nat. Ecol. Evol.* **3**, 274–285 (2019).
95. Guan, Q., Lu, X., Zeng, H., Zhang, Y. & Zhu, J. Heat stress induction of miR398 triggers a regulatory loop that is critical for thermotolerance in *Arabidopsis*. *Plant J.* **74**, 840–851 (2013).
96. Dong, C.-H. et al. Disruption of *Arabidopsis* CHY1 reveals an important role of metabolic status in plant cold stress signaling. *Mol. Plant* **2**, 59–72 (2009).
97. Lee, S. C. et al. Molecular characterization of the submergence response of the *Arabidopsis thaliana* ecotype Columbia. *N. Phytol.* **190**, 457–471 (2011).
98. Cutler, S. R., Rodriguez, P. L., Finkelstein, R. R. & Abrams, S. R. Absciscic acid: emergence of a core signaling network. *Annu. Rev. Plant Biol.* **61**, 651–679 (2010).
99. Yu, Z. et al. How plant hormones mediate salt stress responses. *Trends Plant Sci.* **25**, 1117–1130 (2020).
100. Sánchez-Barrena, M. J., Martínez-Ripoll, M., Zhu, J.-K. & Albert, A. The structure of the *Arabidopsis thaliana* SOS3: molecular mechanism of sensing calcium for salt stress response. *J. Mol. Biol.* **345**, 1253–1264 (2005).
101. Larkin, A. et al. Global land use regression model for nitrogen dioxide air pollution. *Environ. Sci. Technol.* **51**, 6957–6964 (2017).
102. Robertson, K. D. & A. Jones, P. DNA methylation: past, present and future directions. *Carcinogenesis* **21**, 461–467 (2000).
103. Lelieveld, J., Beirle, S., Hörmann, C., Stenchikov, G. & Wagner, T. Abrupt recent trend changes in atmospheric nitrogen dioxide over the Middle East. *Sci. Adv.* **1**, e1500498 (2015).
104. Lamesch, P. et al. The *Arabidopsis* Information Resource (TAIR): improved gene annotation and new tools. *Nucleic Acids Res.* **40**, D1202–D1210 (2012).
105. Xi, Y. & Li, W. BSMAP: whole genome bisulfite sequence MAPPING program. *BMC Bioinformatics* **10**, 232 (2009).
106. Cheng, C.-Y. et al. AraPort11: a complete reannotation of the *Arabidopsis thaliana* reference genome. *Plant J.* **89**, 789–804 (2017).
107. Zilberman, D., Coleman-Derr, D., Ballinger, T. & Henikoff, S. Histone H2A.Z and DNA methylation are mutually antagonistic chromatin marks. *Nature* **456**, 125–129 (2008).
108. Benjamini, Y. & Hochberg, Y. Controlling the false discovery rate: a practical and powerful approach to multiple testing. *J. R. Stat. Soc. Ser. B* **57**, 289–300 (1995).
109. Klepikova, A. V., Kasianov, A. S., Gerasimov, E. S., Logacheva, M. D. & Penin, A. A. A high resolution map of the *Arabidopsis thaliana* developmental transcriptome based on RNA-seq profiling. *Plant J.* **88**, 1058–1070 (2016).

110. Seren, Ü. et al. GWAPP: a web application for genome-wide association mapping in *Arabidopsis*. *Plant Cell* **24**, 4793–4805 (2012).
111. Love, M. I., Huber, W. & Anders, S. Moderated estimation of fold change and dispersion for RNA-seq data with DESeq2. *Genome Biol.* **15**, 550 (2014).
112. Atwell, S. et al. Genome-wide association study of 107 phenotypes in *Arabidopsis thaliana* inbred lines. *Nature* **465**, 627–631 (2010).
113. Yang, J. et al. Genomic inflation factors under polygenic inheritance. *Eur. J. Hum. Genet.* **19**, 807–812 (2011).
114. Devlin, B., Bacanu, S.-A. & Roeder, K. Genomic control to the extreme. *Nat. Genet.* **36**, 1129–1130 (2004).
115. Price, A. L. et al. Principal components analysis corrects for stratification in genome-wide association studies. *Nat. Genet.* **38**, 904–909 (2006).
116. Grimm, D. G. et al. EasyGWAS: a cloud-based platform for comparing the results of genome-wide association studies. *Plant Cell* **29**, 5–19 (2017).
117. Bradbury, P. J. et al. TASSEL: software for association mapping of complex traits in diverse samples. *Bioinformatics* **23**, 2633–2635 (2007).
118. Kisko, M. et al. LPCAT1 controls phosphate homeostasis in a zinc-dependent manner. *eLife* **7**, e32077 (2018).
119. Beavis, W. in *Molecular Dissection of Complex Traits* (ed. Patterson, A. H.) 145–162 (CRC Press, 1998).
120. Xu, S. Theoretical basis of the Beavis effect. *Genetics* **165**, 2259–2268 (2003).
121. Kilian, J. et al. The AtGenExpress global stress expression data set: protocols, evaluation and model data analysis of UV-B light, drought and cold stress responses. *Plant J.* **50**, 347–363 (2007).

Acknowledgements

We thank P. Baduel and V. Colot for sharing SV data, A. Muyle for gbM conservation data and X. Feng, C. Dean, E. Coen and Zilberman lab members for constructive comments on the paper. This work was supported by a European Research Council grant (725746) to D.Z., LUMS Startup grant (STG-188) to Z.S. and US National Science Foundation grant (MCB-2334561) to H.R. This study would not have been possible without *Arabidopsis* 1001 genome, methylome and transcriptome resources.

Author contributions

Z.S. and D.Z. conceived the study; Z.S. performed population genetic analyses and molecular biology experiments; E.H. analysed DNA methylation and gene expression data; J.D.M. analysed DNA methylation data; J.C. generated and analysed DNA methylation and

gene expression data; G.C.-R. and H.R. quantified mineral abundance; M.R.R. performed global statistical analyses of DNA sequence, DNA methylation and gene expression variance; Z.S., E.H. and D.Z. wrote the paper.

Funding

Open access funding provided by Institute of Science and Technology (IST Austria).

Competing interests

The authors declare no competing interests.

Additional information

Extended data is available for this paper at <https://doi.org/10.1038/s41477-025-02108-4>.

Supplementary information The online version contains supplementary material available at <https://doi.org/10.1038/s41477-025-02108-4>.

Correspondence and requests for materials should be addressed to Zaigham Shahzad or Daniel Zilberman.

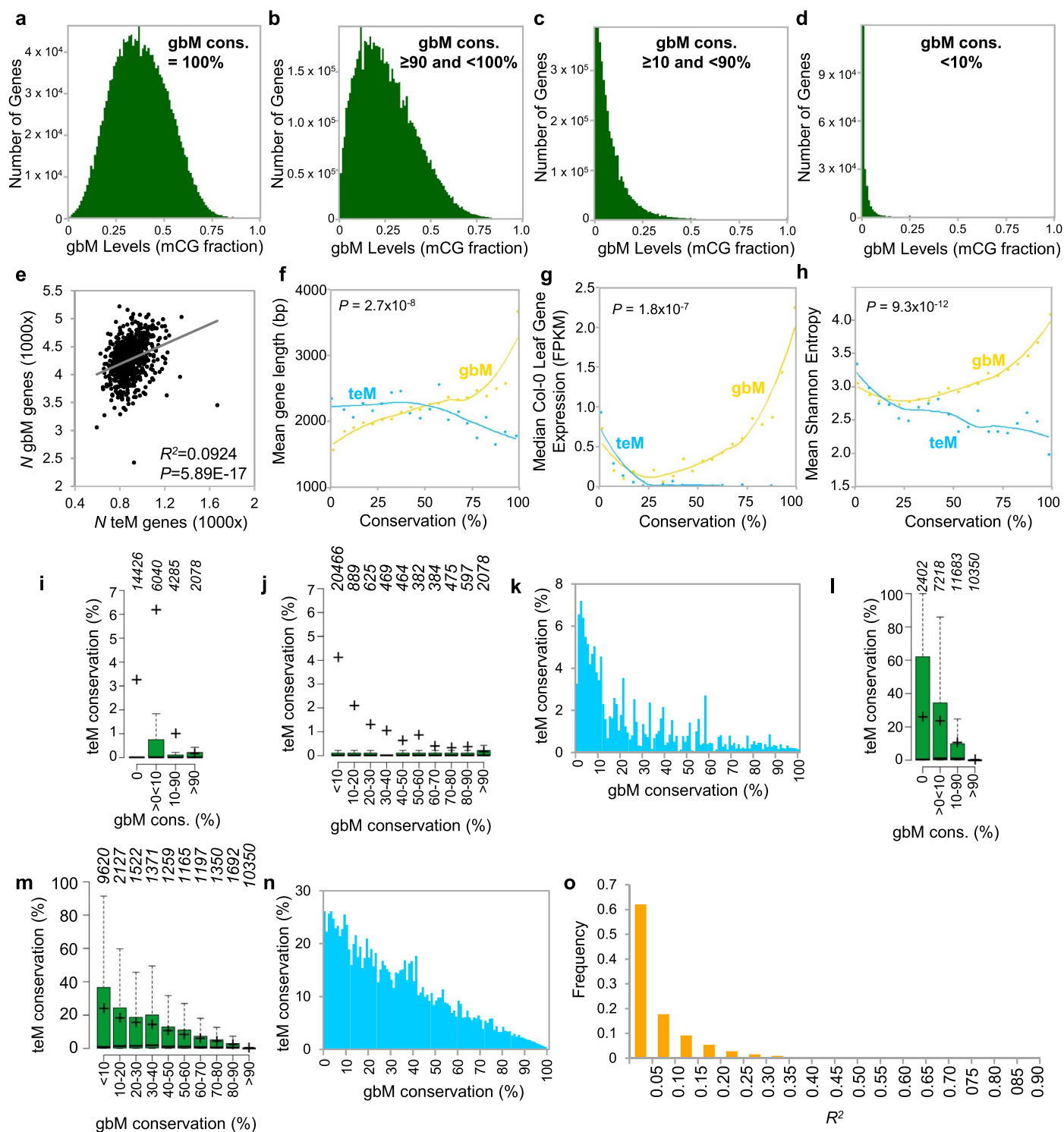
Peer review information *Nature Plants* thanks Bao Liu and the other, anonymous reviewer(s) for their contribution to the peer review of this work.

Reprints and permissions information is available at www.nature.com/reprints.

Publisher's note Springer Nature remains neutral with regard to jurisdictional claims in published maps and institutional affiliations.

Open Access This article is licensed under a Creative Commons Attribution 4.0 International License, which permits use, sharing, adaptation, distribution and reproduction in any medium or format, as long as you give appropriate credit to the original author(s) and the source, provide a link to the Creative Commons licence, and indicate if changes were made. The images or other third party material in this article are included in the article's Creative Commons licence, unless indicated otherwise in a credit line to the material. If material is not included in the article's Creative Commons licence and your intended use is not permitted by statutory regulation or exceeds the permitted use, you will need to obtain permission directly from the copyright holder. To view a copy of this licence, visit <http://creativecommons.org/licenses/by/4.0/>.

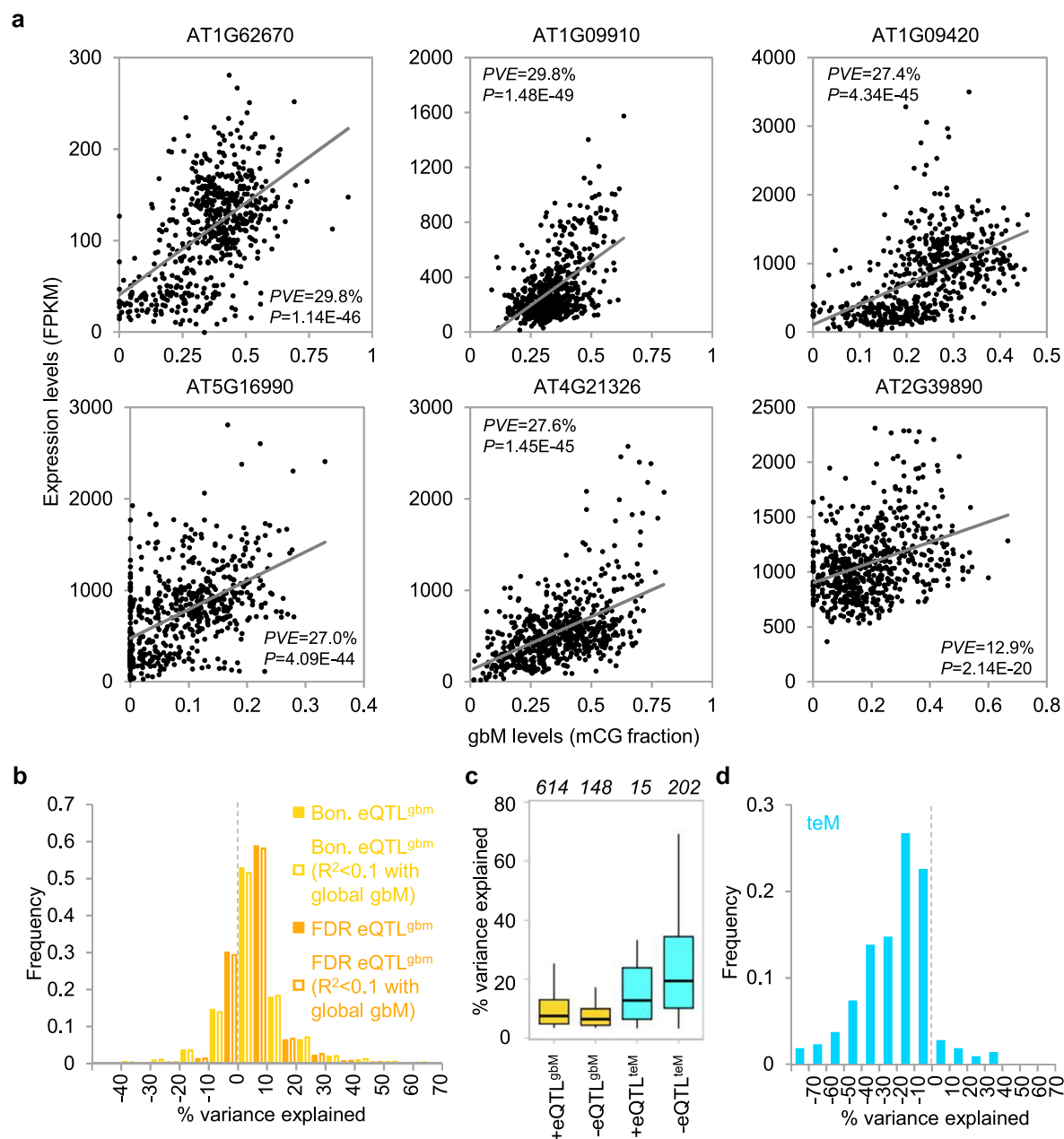
© The Author(s) 2025



Extended Data Fig. 1 | See next page for caption.

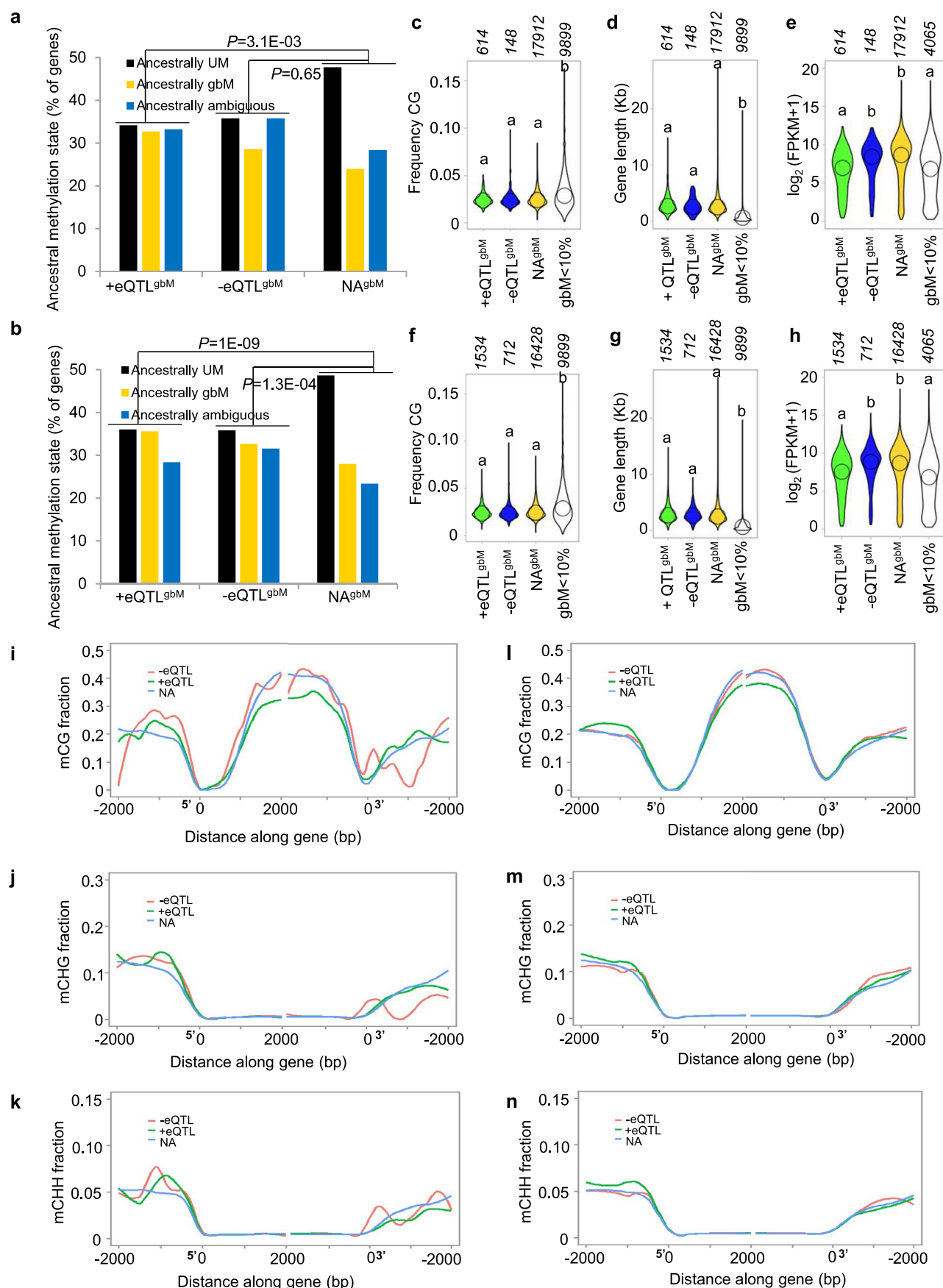
Extended Data Fig. 1 | GbM and teM in *Arabidopsis*. (a–d) Distribution of gbM levels across 948 accessions for genes with 100% gbM population conservation (gbM in all accessions; $N = 1884$; **a**), gbM in ≥ 90 and $< 100\%$ of accessions ($N = 8119$; **b**), gbM in ≥ 10 and $< 90\%$ of accessions ($N = 10,165$; **c**), and gbM in $< 10\%$ of accessions ($N = 4973$; **d**). Only genes with > 20 CG sites are included. (e) Pearson's correlation analysis between the number (N) of gbM and teM genes in accessions using published definitions of gbM and teM⁶⁰. (f–h) Characteristics of genes binned by their gbM (gold) and teM (blue) frequencies: mean length in bp (f), median expression in Col-0 leaf RNA-seq data⁵⁴ (g) and Shannon entropy¹⁰⁹ (h). A linear model was used to associate gbM or teM population frequencies with the gene characteristics. P -values are for comparisons of gbM vs. teM associations using a two-sided F-test. (i–k) Conservation of teM epialleles in published⁶⁰ gbM conservation categories (i, four gbM classes; j, decile gbM bins; k, percentile gbM bins). Analysis across three gbM conservation bins ($< 10\%$, 10 – 90% , and $> 90\%$) led to the published conclusion

that teM frequency increases with gbM frequency⁶⁰. However, we noted that the published $< 10\%$ category contains only UM genes. Categorizing the published data⁶⁰ in various ways (i–k) shows that teM prevalence decreases with increasing gbM. These results are broadly consistent with those obtained with our gbM and teM definitions: (l; four gbM classes), (m; decile gbM bins), and (n; percentile gbM bins). The numbers above box plots indicate the number of genes in each category, center lines represent sample medians, and plus signs correspond to means. Box limits indicate the 25th and 75th percentiles; whiskers extend to 1.5 times the interquartile range. Note that the numbers of genes in gbM conservation bins in panels l and m are different from those in Fig. 1b because only genes with epigenetic state calls in $> 70\%$ of accessions are included in Fig. 1b, whereas this cutoff is not applied here. (o) Frequency distribution of correlation (R^2) between gbM levels of individual genes and global gbM levels of accessions. A linear model is used to estimate R^2 .



Extended Data Fig. 2 | Association between gbM, teM and expression of *Arabidopsis* genes. (a) GbM and expression of six example genes across accessions. Percent expression variance explained (PVE) by gbM and P values of Pearson's correlation tests are indicated. (b) Frequency distribution of percent expression variance of Bonferroni $\alpha = 0.05$ and FDR 0.05 eQTL^{gbM} genes explained by mCG variation. The filled bars depict all eQTL^{gbM} genes significant at respective thresholds, and the empty bars represent eQTL^{gbM} genes showing

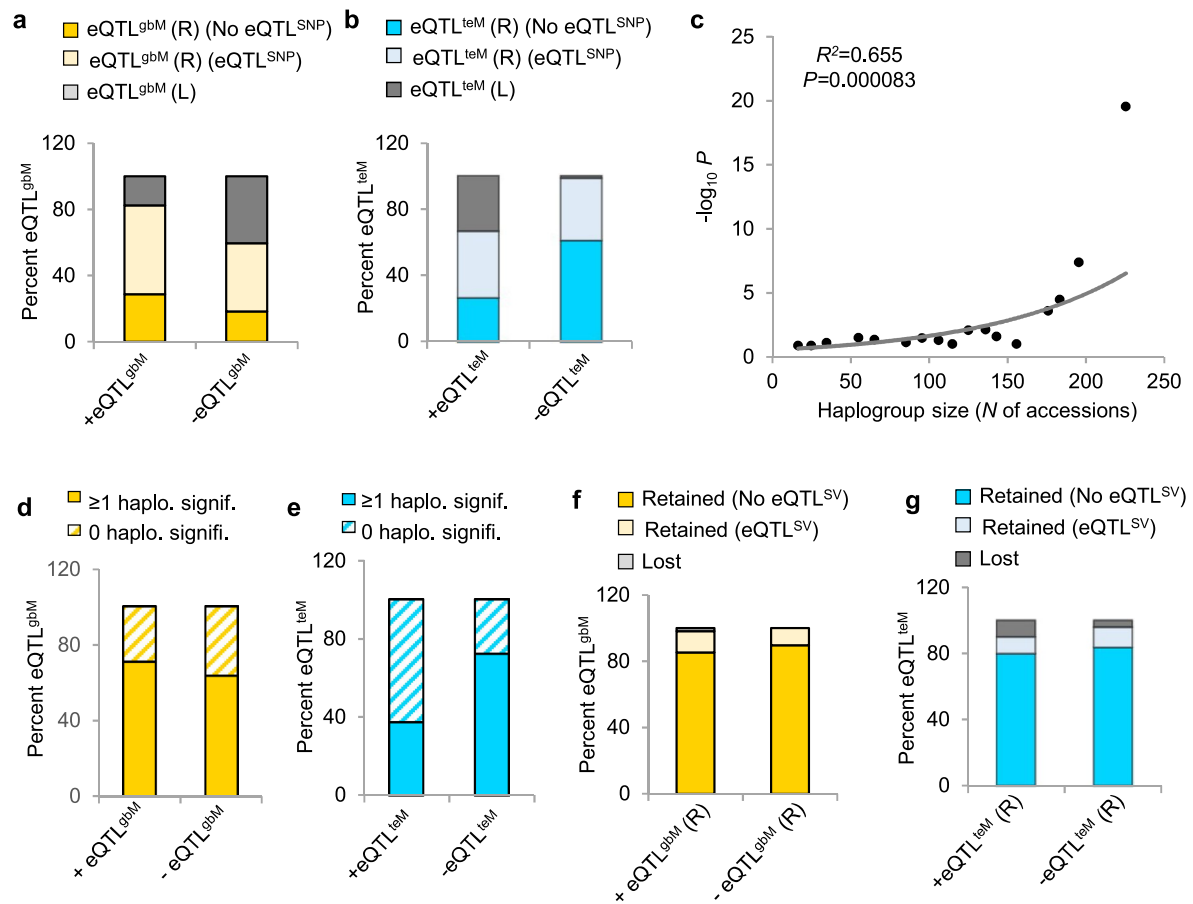
$R^2 < 0.1$ between local and global gbM levels. (c) Percent expression variance explained by gbM or teM in Bonferroni eQTL^{gbM/teM} genes. The number of QTLs corresponding to each category is indicated. Center lines represent sample medians, box limits indicate the 25th and 75th percentiles, whiskers extend to 1.5 times the interquartile range. (d) Frequency distribution of percent expression variance of Bonferroni eQTL^{teM} genes explained by mCG variation.



Extended Data Fig. 3 | See next page for caption.

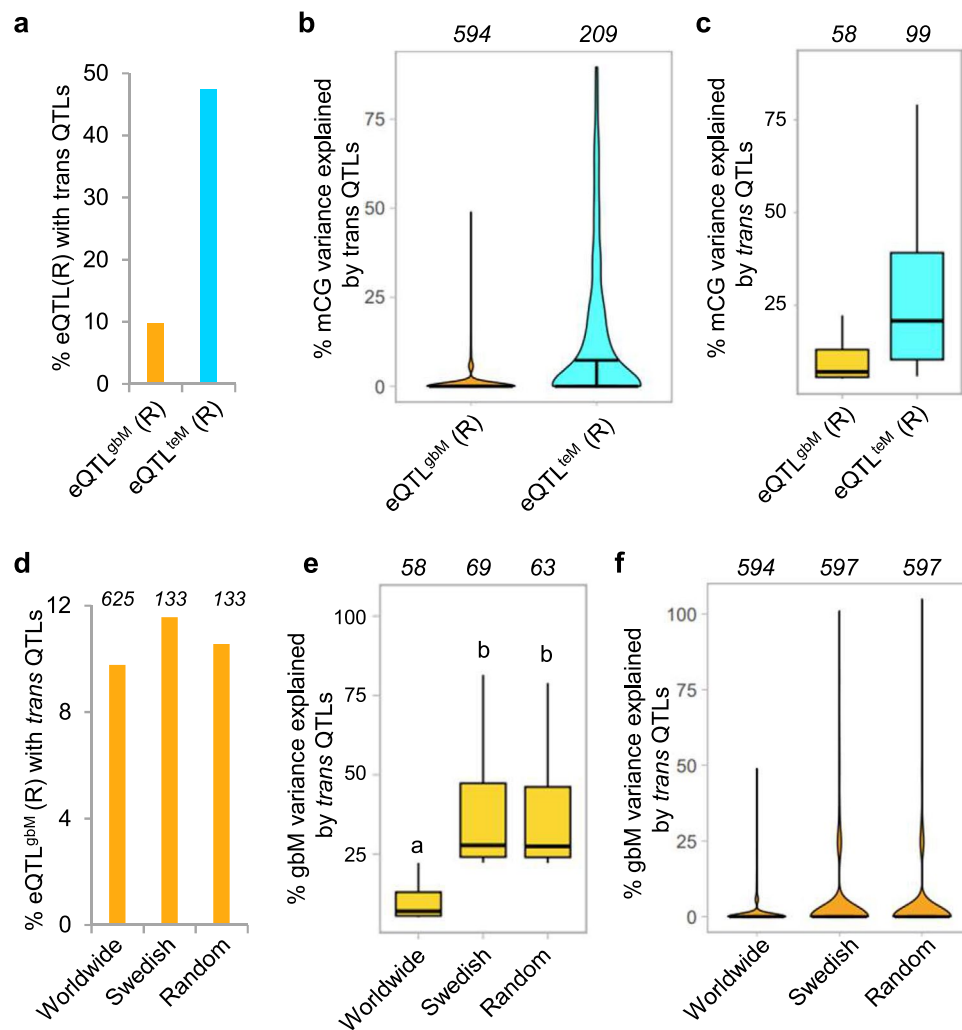
Extended Data Fig. 3 | Characteristics of eQTL gbM genes. (a–b) Ancestral methylation states of +eQTL^{gbM}, -eQTL^{gbM}, and NA^{gbM} genes using the Bonferroni (a) or FDR 0.05 (b) classification. Ancestral methylation states were determined by analyzing methylation states of *Arabidopsis thaliana* orthologs in *Arabidopsis lyrata* and *Capsella rubella* and retrieved from⁵¹. *P* values correspond to chi-squared test. (c–h) Plots show CG dinucleotide frequency (c and f), gene length (d and g), and gene expression (e and h) of Bonferroni (c–e) or FDR 0.05 (f–h)

eQTL^{gbM} genes, NA^{gbM} (non-associated) genes, and genes with gbM in <10% of accessions. Different letters signify $P < 0.001$, one-way ANOVA, Dunn's test. Numbers of genes within each group are indicated. (i–n) Methylation in the CG (i and l), CHG (j and m) and CHH (k and n) contexts within and adjacent to +eQTL^{gbM}, -eQTL^{gbM} and NA^{gbM} genes using the Bonferroni (i–k) or FDR 0.05 (l–n) classifications.



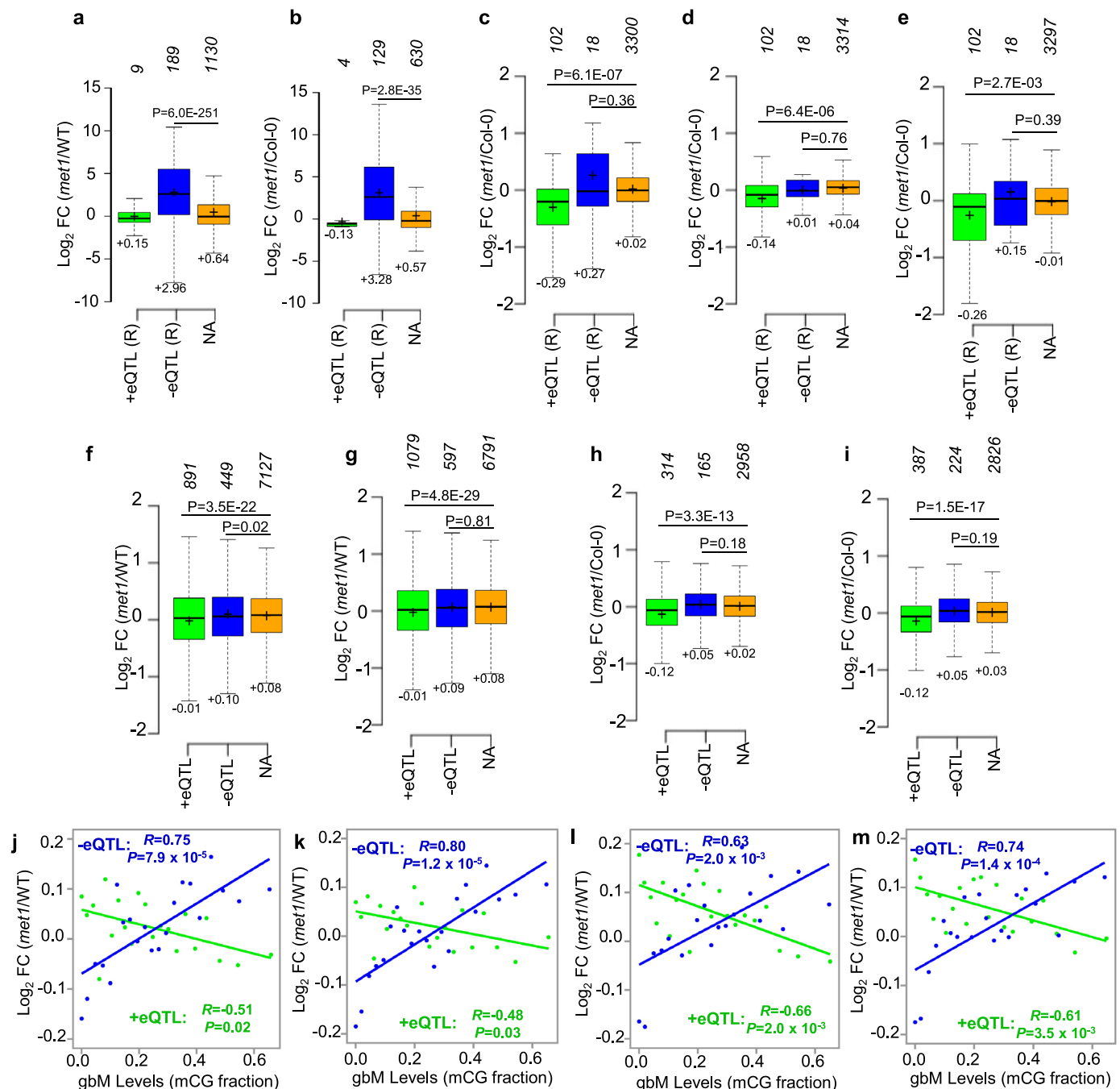
Extended Data Fig. 4 | Most eQTL^{gbM/teM} gene expression effects are independent of local SNP variation. (a and b) Frequency of retained (R) or lost (L) eQTL^{gbM} (a) and eQTL^{teM} (b) genes after accounting for expression GWA SNPs. (c) Loss of statistical power for association analyses in haplogroups due to decreasing population size. The $-\log_{10} P$ values for associations between gbM/teM and gene expression exhibit an exponential increase with respect to the number of accessions in haplogroups. Indicated R^2 and P values correspond to

exponential regression. (d and e) Frequency of eQTL^{gbM} (d) and eQTL^{teM} (e) genes with a significant association between mCG and gene expression in at least one haplogroup. Despite reduced statistical power (c) in SNP invariant haplogroups due to smaller population sizes, significant associations between gbM variation and expression are detected for a majority of eQTL^{gbM} genes. (f and g) Frequency of retained or lost eQTL^{gbM} (f) and eQTL^{teM} (g) genes after accounting for structural variation (SV) effects on expression.



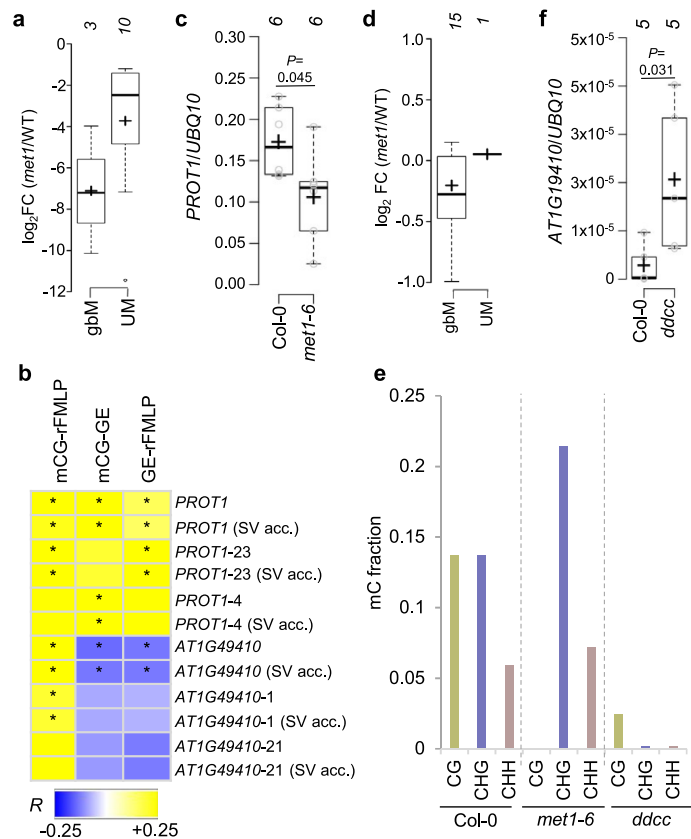
Extended Data Fig. 5 | Trans genetic variation explains a minor fraction of gbM. (a) Percentage of eQTL^{gbM/teM} retained (R) genes that have *trans* genetic QTLs associated with the variation of gbM or teM. (b) Average effects (\pm standard error) of *trans* polymorphism on mCG variation in all retained eQTL^{gbM/teM} genes, with number of QTLs indicated. (c) Effect sizes of *trans* polymorphism on mCG variation of retained eQTL^{gbM/teM} genes having *trans* QTLs. Center lines represent sample medians, box limits indicate the 25th and 75th percentiles, whiskers extend to 1.5 times the interquartile range. The number of QTLs corresponding to each class is indicated above the plots. (d) Percentage of retained eQTL^{gbM} having *trans* QTLs in the entire worldwide population, a published Swedish population⁵⁰,

and a random population of equal size to the Swedish population. Numbers of accessions in each panel are indicated. (e) Effect sizes of *trans* genetic polymorphisms on gbM variation of retained eQTL^{gbM} genes having *trans* QTLs in worldwide, Swedish, and random populations. Box plots as in c. Different letters signify $P < 0.05$, one-way ANOVA, Tukey's test. (f) Average effects (\pm standard error) of *trans* genetic variation on gbM variation of all retained eQTL^{gbM} genes in worldwide, Swedish, and random populations, with number of genes indicated. Note the inflation of estimated *trans* effects in the smaller populations, a phenomenon known as the Beavis effect^{119,120}.



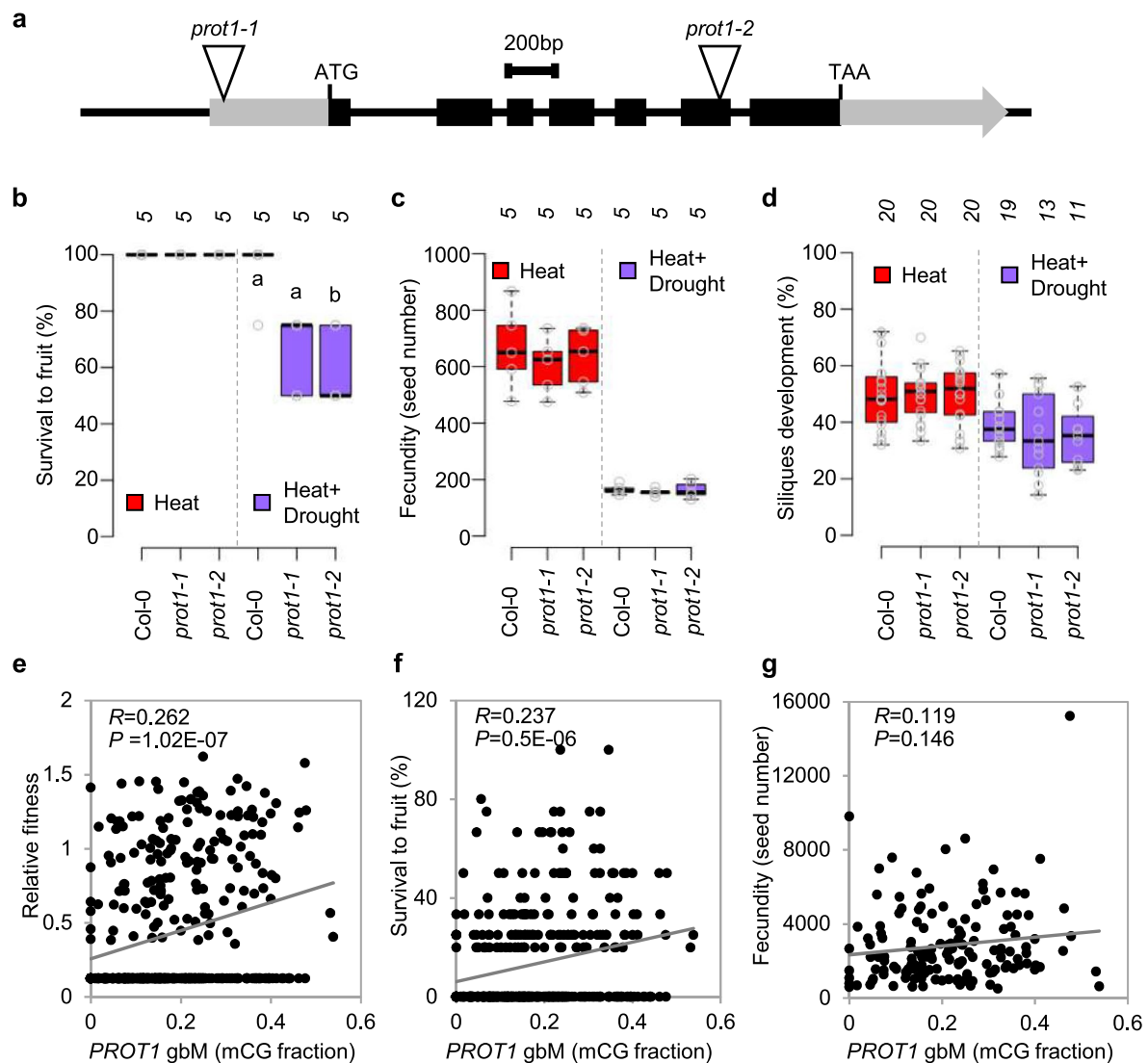
Extended Data Fig. 6 | GBM quantitatively affects gene expression. (a and b) Expression in *met1* compared to WT of Bonferroni ($\alpha = 0.05$) eQTL^{tem} genes retained (R) after accounting for genetic variation in seedlings across 16 accessions⁷⁵ (a) and different tissues of Col-0 (leaf, seedling and inflorescence^{54,77}; b). (c-e) Expression in *met1* compared to Col-0 of Bonferroni ($\alpha = 0.05$) eQTL^{gbM} genes retained (R) after accounting for genetic variation in either leaf (c), inflorescence (d) or seedling (e). (f and g) Expression in *met1* compared to WT seedlings of FDR 0.01 (f) and FDR 0.05 (g) eQTL^{gbM} genes across 16 accessions. (h and i) Expression in *met1* compared to WT of FDR 0.01 (h) and FDR 0.05 (i) eQTL^{gbM} genes in different tissues of Col-0 (leaf, seedling and inflorescence). Center lines within box plots represent sample medians, plus signs correspond

to means and are noted below the plots. Box limits indicate the 25th and 75th percentiles, whiskers extend to 1.5 times the interquartile range. Numbers of genes within each group are noted above the plots. P , two-tailed Student's t -test between indicated group and NA (non-associated) genes. (j-m) Relationship between gbM levels of retained +eQTL and -eQTL genes using the FDR 0.01 (j and l) or FDR 0.05 (k and m) groups in WT plants across 16 accessions⁷⁵ and \log_2 fold expression change in *met1* compared to WT of that accession. Genes with mCG >5% and/or non-CG methylation >1% in the putative promoter (2 kb upstream or up to the nearest upstream gene, whichever is shorter) were excluded in l and m. Genes were grouped by gbM levels. R and P values correspond to Pearson's correlation.



Extended Data Fig. 7 | Methylation and expression of epigenetic flowering and relative fitness QTLs. (a) *FLC* expression change in *met1* lines of accessions with either gbM or unmethylated (UM) *FLC* epialleles in wild-type (WT), assessed by RNA-seq⁷⁵. Numbers of accessions within each group are indicated. **(b)** Tripartite association between intragenic DNA methylation (mCG), gene expression (GE), and relative MLP fitness (rFMLP) in the entire population and after accounting (acc.) for structural variation (SV). Associations between the three variables are shown in two independent haplogroups of *PROT1* (*PROT1-23* and *PROT1-4*) and *AT1G19410* (*AT1G19410-1* and *AT1G19410-21*) before and after accounting for SV. **P* < 0.05, Pearson's correlation test. **(c)** Transcript levels of *PROT1* relative to *UBQ10* in Col-0 and *met1-6*, assessed by qRT-PCR in six biological replicates.

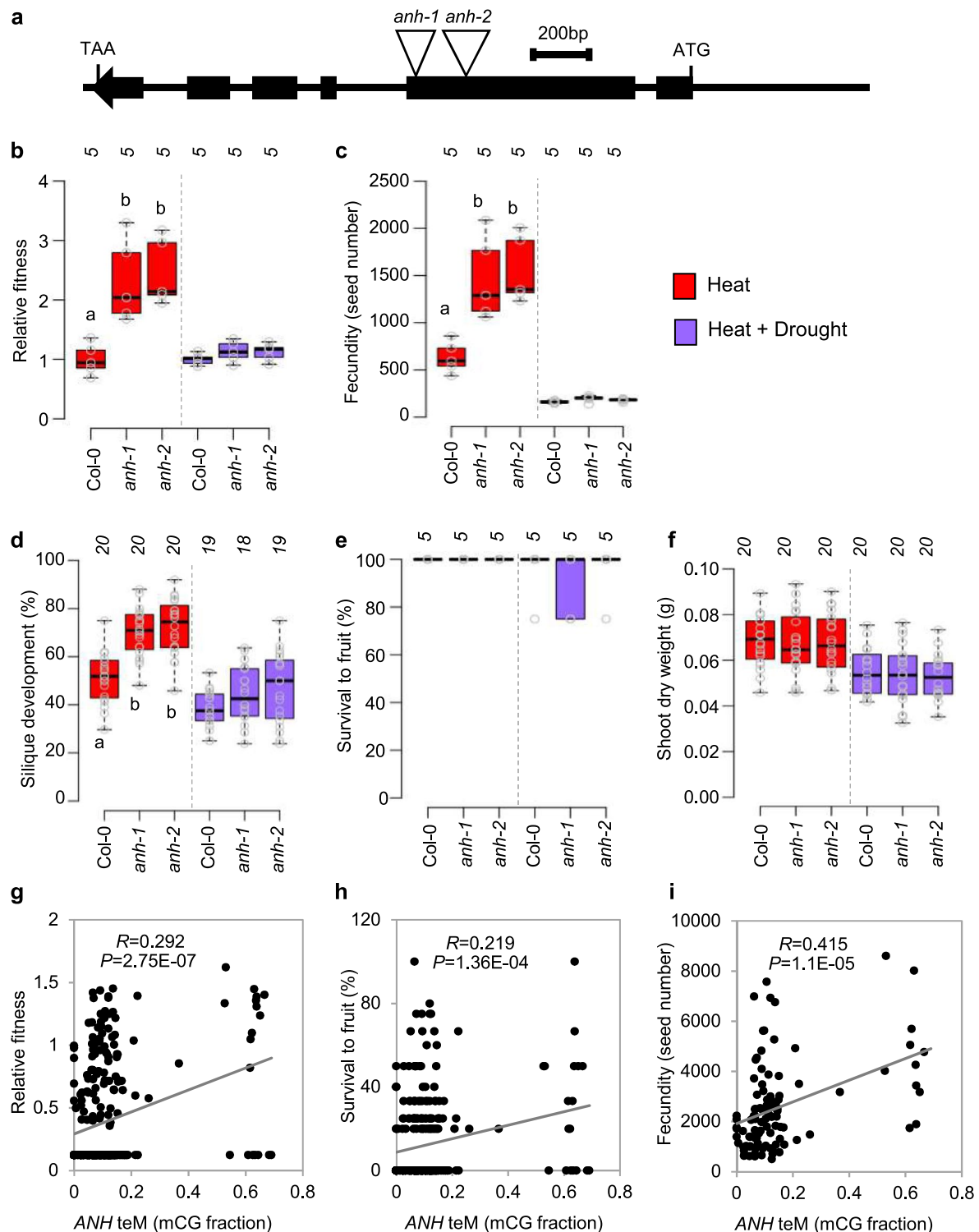
P, two-tailed Student's t-test. **(d)** *PROT1* expression change in *met1* lines of accessions with either gbM or UM *PROT1* epialleles in WT, assessed by RNA-seq⁷⁵. Numbers of accessions within each group are indicated. **(e)** DRM and CMT methyltransferases control teM of *AT1G19410*. Fractional methylation in CG, CHG, and CHH sequence contexts is shown in indicated genotypes. **(f)** Transcript levels of *AT1G19410* (*ANH*) relative to *UBQ10* in Col-0 and *ddcc*, assessed by qRT-PCR in five biological replicates. *P*, two-tailed Student's t-test. Center lines within box plots represent sample medians and plus signs correspond to means. Box limits indicate the 25th and 75th percentiles, whiskers extend to 1.5 times the interquartile range.



Extended Data Fig. 8 | *PROT1* promotes fitness under heat and drought stress.

(a) Schematic representation of *PROT1* genomic regions with positions of the T-DNA insertions. (b–d) Box plots showing survival to fruit (b), fecundity (c), and fertility (% of flowers developing siliques; d) phenotypes of *prot1* mutant and Col-0 wild type plants under heat stress (red) or combined heat and drought stress (purple). Numbers of independent experiments are indicated for survival

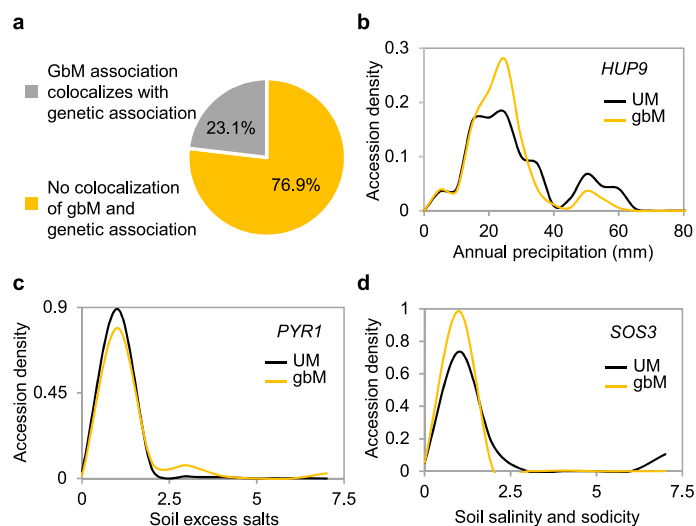
to fruit (b) and fecundity (c). Numbers of plants are indicated for fertility (d). Box boundaries indicate the 25th and 75th percentiles, whiskers extend to 1.5 times the interquartile range, center lines correspond to medians. Different letters signify $P < 0.05$, one-way ANOVA, Tukey's test. (e–g) Association of *PROT1* gbM with relative fitness (e), survival to fruit (f), and fecundity (g). Correlation coefficients (R) and P values of Pearson's correlation test are indicated.



Extended Data Fig. 9 | AT1G19410 (*ANH*) reduces fertility under heat stress.

(a) Schematic representation of *ANH* genomic region with positions of the T-DNA insertions. (b–f) Box plots show relative fitness (b), fecundity (c), fertility (d), survival to fruit (e), and shoot dry weight (f) of *anh* mutants (two independent alleles) relative to Col-0 under heat stress (red) or joint heat and drought stress (purple). Numbers of independent experiments are indicated for relative fitness (b), fecundity (c), and survival to fruit (e). Numbers of plants are indicated for

fertility (d) and shoot weight (f). Box boundaries indicate the 25th and 75th percentiles, whiskers extend to 1.5 times the interquartile range, center lines correspond to medians. Different letters signify $P < 0.05$, one-way ANOVA, Tukey's test. (g–i) Association of *ANH* teM with relative fitness (g), survival to fruit (h), and fecundity (i). Correlation coefficients (R) and P values of Pearson's correlation analysis are indicated.



Extended Data Fig. 10 | Associations between gbM variation and the environment. (a) Frequency of associations between gbM and environmental data colocating with genetic associations. (b–d) Associations between gbM and environmental data for *HUP9* (b), *PYR1* (c), and *SOS3* (d).

Reporting Summary

Nature Portfolio wishes to improve the reproducibility of the work that we publish. This form provides structure for consistency and transparency in reporting. For further information on Nature Portfolio policies, see our [Editorial Policies](#) and the [Editorial Policy Checklist](#).

Statistics

For all statistical analyses, confirm that the following items are present in the figure legend, table legend, main text, or Methods section.

n/a	Confirmed
<input type="checkbox"/>	<input checked="" type="checkbox"/> The exact sample size (<i>n</i>) for each experimental group/condition, given as a discrete number and unit of measurement
<input type="checkbox"/>	<input checked="" type="checkbox"/> A statement on whether measurements were taken from distinct samples or whether the same sample was measured repeatedly
<input type="checkbox"/>	<input checked="" type="checkbox"/> The statistical test(s) used AND whether they are one- or two-sided <i>Only common tests should be described solely by name; describe more complex techniques in the Methods section.</i>
<input type="checkbox"/>	<input checked="" type="checkbox"/> A description of all covariates tested
<input type="checkbox"/>	<input checked="" type="checkbox"/> A description of any assumptions or corrections, such as tests of normality and adjustment for multiple comparisons
<input type="checkbox"/>	<input checked="" type="checkbox"/> A full description of the statistical parameters including central tendency (e.g. means) or other basic estimates (e.g. regression coefficient) AND variation (e.g. standard deviation) or associated estimates of uncertainty (e.g. confidence intervals)
<input type="checkbox"/>	<input checked="" type="checkbox"/> For null hypothesis testing, the test statistic (e.g. <i>F</i> , <i>t</i> , <i>r</i>) with confidence intervals, effect sizes, degrees of freedom and <i>P</i> value noted <i>Give P values as exact values whenever suitable.</i>
<input type="checkbox"/>	<input checked="" type="checkbox"/> For Bayesian analysis, information on the choice of priors and Markov chain Monte Carlo settings
<input type="checkbox"/>	<input checked="" type="checkbox"/> For hierarchical and complex designs, identification of the appropriate level for tests and full reporting of outcomes
<input type="checkbox"/>	<input checked="" type="checkbox"/> Estimates of effect sizes (e.g. Cohen's <i>d</i> , Pearson's <i>r</i>), indicating how they were calculated

Our web collection on [statistics for biologists](#) contains articles on many of the points above.

Software and code

Policy information about [availability of computer code](#)

Data collection	No software was used in data collection.
Data analysis	Analysis of methylation data: BSMAP (v2.90) Analysis of RNA-seq data: HiSat2 (v2.11.2), samtools (v1.18), Further analysis of bisulfite and RNA-seq data, statistical analyses and creation of plots: R, including additional packages ggplot2 (v3.4.1), Rsubread (v2.12.3), DESeq2 (v1.38.3), dplyr (v1.1.1), GenomicRanges (v1.50.2), data.table (v1.14.8), matrixStats (v0.63.0), scales (v1.2.1), tidyr (v1.3.0) Fitting of a regression model - Trejo Banos et al., 2020 Correlation analysis: SigmaPlot 1.0 epiGWAS: MLM and GLM implemented in TASSEL, AMM implemented in PyGWAS (1.7.4)

For manuscripts utilizing custom algorithms or software that are central to the research but not yet described in published literature, software must be made available to editors and reviewers. We strongly encourage code deposition in a community repository (e.g. GitHub). See the Nature Portfolio [guidelines for submitting code & software](#) for further information.

Data

Policy information about [availability of data](#)

All manuscripts must include a [data availability statement](#). This statement should provide the following information, where applicable:

- Accession codes, unique identifiers, or web links for publicly available datasets
- A description of any restrictions on data availability
- For clinical datasets or third party data, please ensure that the statement adheres to our [policy](#)

Newly generated RNA-seq and bisulfite sequencing data are available at GEO under accession number GSE183785.

Research involving human participants, their data, or biological material

Policy information about studies with [human participants or human data](#). See also policy information about [sex, gender \(identity/presentation\), and sexual orientation](#) and [race, ethnicity and racism](#).

Reporting on sex and gender

Reporting on race, ethnicity, or other socially relevant groupings

Population characteristics

Recruitment

Ethics oversight

Note that full information on the approval of the study protocol must also be provided in the manuscript.

Field-specific reporting

Please select the one below that is the best fit for your research. If you are not sure, read the appropriate sections before making your selection.

☒ Life sciences ☐ Behavioural & social sciences ☐ Ecological, evolutionary & environmental sciences

For a reference copy of the document with all sections, see [nature.com/documents/nr-reporting-summary-flat.pdf](https://www.nature.com/documents/nr-reporting-summary-flat.pdf)

Life sciences study design

All studies must disclose on these points even when the disclosure is negative.

Sample size

Data exclusions

Replication

Randomization

Blinding

Reporting for specific materials, systems and methods

We require information from authors about some types of materials, experimental systems and methods used in many studies. Here, indicate whether each material, system or method listed is relevant to your study. If you are not sure if a list item applies to your research, read the appropriate section before selecting a response.

Materials & experimental systems

n/a	Involvement in the study
<input checked="" type="checkbox"/>	<input type="checkbox"/> Antibodies
<input checked="" type="checkbox"/>	<input type="checkbox"/> Eukaryotic cell lines
<input checked="" type="checkbox"/>	<input type="checkbox"/> Palaeontology and archaeology
<input checked="" type="checkbox"/>	<input type="checkbox"/> Animals and other organisms
<input checked="" type="checkbox"/>	<input type="checkbox"/> Clinical data
<input checked="" type="checkbox"/>	<input type="checkbox"/> Dual use research of concern
<input type="checkbox"/>	<input checked="" type="checkbox"/> Plants

Methods

n/a	Involvement in the study
<input checked="" type="checkbox"/>	<input type="checkbox"/> ChIP-seq
<input checked="" type="checkbox"/>	<input type="checkbox"/> Flow cytometry
<input checked="" type="checkbox"/>	<input type="checkbox"/> MRI-based neuroimaging

Plants

Seed stocks	Seeds were obtained from the Nottingham Arabidopsis Stock Centre (NASC) and the Arabidopsis Biological Resource Center (ABRC) as described in Methods
Novel plant genotypes	None
Authentication	None required